

1                   **Measuring and modeling mercury in the atmosphere: A critical review**

2

3

4                   Mae Sexauer Gustin<sup>1</sup>, Helen M. Amos<sup>2</sup>, Jiaoyan Huang<sup>1</sup>, Matthieu B. Miller<sup>1</sup>, Keith Heidecorn<sup>1</sup>

5

6                   <sup>1</sup>Department of Natural Resources and Environmental Science, University of Nevada-Reno,  
7                   Reno, NV, US 89557

8                   <sup>2</sup>Department of Environmental Health, Harvard School of Public Health, Boston, Massachusetts,  
9                   US, 02115

10

11

12

13

14

15

16

17

18

19

20

21

22

23

24     **Abstract**

25           Measurements of atmospheric mercury (Hg) are being increasingly incorporated into  
26   monitoring networks worldwide. These data are expected to support and inform regulatory  
27   decision making aimed at protecting human and wildlife health. Here we critically review current  
28   efforts to measure Hg concentrations in the atmosphere, summarize uncertainties in current  
29   methods, and describe how these impact models. There are three operationally defined forms of  
30   atmospheric Hg: gaseous elemental mercury (GEM), gaseous oxidized mercury (GOM), and  
31   particulate bound mercury (PBM). There is relative confidence in GEM measurements, but  
32   GOM and PBM are less well understood. Field and laboratory investigations suggest the  
33   methods to measure GOM and PBM are impacted by analytical interferences that vary with  
34   environmental setting (e.g., ozone, relative humidity), and GOM concentrations can be biased  
35   low by a factor of 1.6 to 12 depending on the chemical composition of GOM. The composition  
36   of GOM (e.g.,  $\text{HgBr}_2$ ,  $\text{HgCl}_2$ ,  $\text{HgBrOH}$ ) varies across space and time. This has important  
37   implications for refining existing measurement methods and developing new ones,  
38   model/measurement comparisons, model development, and assessing trends. In addition, unclear  
39   features of previously published data may now be re-examined and possibly explained, which is  
40   demonstrated through a case study. We recommend applying a factor of 3 as a conservative  
41   correction to reported GOM concentrations. Priorities for future research include identification of  
42   GOM compounds in ambient air, and development of information on their chemical and physical  
43   properties. With this information identification of redox mechanisms and associated rate  
44   coefficients may be developed. A GOM calibration system should be developed that contains  
45   the most abundant chemical compounds in the air.

46     **1. Introduction**

47        The Minamata Convention for mercury (Hg) has been signed by more than 120 nations  
48    and is now being ratified. The primary objective of the Convention is to “protect human health  
49    and the environment from anthropogenic emissions and releases of mercury and mercury  
50    compounds” (UNEP Minamata Convention, 2014). A key challenge for Hg researchers is  
51    developing linkages between Hg in the atmosphere, deposition, and ecosystem contamination  
52    (Pirrone et al., 2013). Here we review where the science on measuring and modeling  
53    atmospheric Hg currently stands, and offer suggestions for future research directions that will  
54    both advance understanding of Hg cycling in and between the Earth’s spheres, and better serve  
55    the needs of the Convention.

56        Although the atmosphere is a relatively minor reservoir of Hg compared to the ocean or  
57    soils, it is an important pathway by which Hg is distributed globally over short timescales (on the  
58    order of 1 year). Atmospheric deposition represents the major pathway of Hg input to terrestrial  
59    and aquatic ecosystems outside areas of direct contamination. A variety of environmental  
60    archives, including remote lake sediments, ombrotrophic peat bogs, glacial ice, and tree rings  
61    suggest Hg inputs to the atmosphere have increased several-fold in the last 150 years (cf.  
62    Engstrom et al., 2014; Schuster et al., 2002; Wright et al., 2014b). Direct observations of  
63    atmospheric Hg suggest concentrations have been decreasing over the last ~15 years (Slemr et  
64    al., 2011; Cole and Steffen, 2010; Soerensen et al., 2012; Cole et al., 2010; 2014), despite trends  
65    in global anthropogenic emissions being relatively flat or increasing (AMAP/UNEP, 2013). This  
66    unexpected decrease remains unexplained, and underscores the need to continue monitoring and  
67    studying Hg in the atmosphere.

68        Atmospheric Hg is operationally defined as gaseous elemental Hg (GEM), gaseous  
69    oxidized Hg (GOM), and particulate bound Hg (PBM) (Lindberg et al., 2007; Schroeder and

70 Munthe, 1998; Landis et al., 2002). Previously it was thought that GEM was 95-99% of Hg in  
71 the atmosphere (cf. Schroeder and Munthe, 1998). Recent work is pointing towards GOM being  
72 25% of total Hg in the boundary layer (see the discussion below). In the Arctic, 100%  
73 conversion of GEM to GOM has been observed (Steffan et al., 2014; 2015); however, this is not  
74 always the case and depends on the sampling location. Measuring the forms of Hg in the  
75 atmosphere is difficult. Mixing ratios of GEM, GOM, and PBM are all at low parts per  
76 quadrillion by volume ( $\text{ng m}^{-3}$  and  $\text{pg m}^{-3}$ ). In addition, there are different GOM compounds in  
77 the air (Huang et al., 2013; this issue). Thus, GOM and PBM have complex fundamental  
78 physiochemical properties. Because of the complexity, recent work has combined GOM and  
79 PBM concentrations as measured by the Tekran® system and defined this as reactive Hg  
80 (RM=GOM+PBM).

81 Here we review current methods for measuring the forms of Hg in the atmosphere and  
82 models used to interpret these data. The advantages and limitations of each measurement method  
83 are discussed, and a narrative is provided on how we have arrived at our current understanding of  
84 the limitations. The number of models that have developed the capacity to simulate atmospheric  
85 Hg has multiplied in the last decade. We review major gains in Hg science gleaned from the use  
86 of measurements and models together, as well as key open questions. We conclude with a  
87 discussion of outstanding problems facing measurement and modeling communities.

88

89 ***2. Methods for measuring atmospheric Hg***

90 **2.1 Atmospheric mercury basics**

91 Ambient GEM concentrations are on the order of a few  $\text{ng m}^{-3}$  while GOM and PBM  
92 have been considered to be two-to-three orders smaller (cf. Valente et al., 2007). Current

93 research, described herein, is demonstrating RM can make up 25% of Hg in the planetary  
94 boundary layer. Mercury is typically detected by atomic absorption (AAS) or atomic  
95 fluorescence spectroscopy (AFS). In nearly all cases, the Hg forms are pre-concentrated on gold-  
96 coated surfaces, because the sensitivity of AAS and AFS is, with the exception of laser  
97 techniques, not sufficient for direct measurements of Hg at ambient concentrations. GOM and  
98 PBM are converted to GEM by thermal desorption from the gold surfaces. Gold is the most  
99 frequently used and best-studied pre-concentration material for Hg, but can become passivated  
100 (see Huang et al., 2014; Landis et al., 2000). The Tekran® 2537/1130/1135 system is the most  
101 widely adopted method by the international community of scientists, and has been incorporated  
102 into monitoring networks such as the Canadian Mercury Network (CAMNet), Atmospheric  
103 Mercury Network (AMNet), and Global Mercury Observation System (GMOS). Alternate  
104 measurement methods have been developed, but are currently operated on a limited scale.

105 An AAS or AFS instrument combined with a pre-concentration on a gold adsorber with a  
106 pyrolyzer in-line will provide total gaseous mercury (TGM=GEM + GOM) or total atmospheric  
107 mercury (TAM=GEM + GOM + PBM). If sampling for GOM, since it is adhesive, sampling  
108 lines should be designed to prevent wall loss (short and/or heated).

109 GOM and PBM are in temperature dependent equilibrium (Rutter and Schauer, 2007).  
110 Specific PBM sampling has to take account of this, in addition to the usual precautions to  
111 prevent size dependent particle losses. Since it is difficult to achieve separation of PBM and  
112 GOM without disturbing the equilibrium, RM is a more accurate measurement to use. Due to  
113 lack of capture of GOM by the denuder and collection on the PBM unit, discussion of RM is  
114 more realistic. (We thank Dr. Franz Slemr for suggestions for this paragraph, see ACP review  
115 comments, March 8, 2015).

116

117 **2.2 Active Automated systems**

118 *2.2.1 Tekran® system*

119 The Tekran® 2537/1130/1135 system has been widely used to measure atmospheric Hg  
120 for the past ~15 years (Landis et al., 2002). The Tekran® 2537 module measures TGM or GEM  
121 in  $\text{ng m}^{-3}$  and was the first component to be developed. The 1130 and 1135 components were  
122 added to this system to measure GOM and PBM in  $\text{pg m}^{-3}$  (Landis et al., 2002), respectively. The  
123 instrument pulls air through an elutriator that is heated to 50°C and removes particles  $> 2.5 \mu\text{m}$ ,  
124 depending on the flow rate (Lyman et al., 2010). This particle size cut is necessary to keep larger  
125 particles from depositing on the denuder. GOM is collected on a potassium chloride (KCl)-  
126 coated denuder, and PBM on a column of quartz chips and a quartz filter. Air passes through 10  
127 m of heated line with a soda lime trap and Teflon filter at the 2537 inlet, and then into the 2537  
128 where GEM is collected on a gold trap. It is not known whether the soda lime trap captures and  
129 retains GOM. GOM (500°C) and PBM (800°C) are thermally desorbed from their collection  
130 surfaces, loaded on the gold traps, and quantified as GEM (gold traps are heated to 350°C) by  
131 cold vapor atomic fluorescence spectrometry (CVAFS). Although the particle cut inlet, coated  
132 annular denuder, particle filtration device, and heated line are all held at constant temperatures  
133 (50°C) when sampling, there are temperature drops within the sampling line and GOM may be  
134 lost to the walls (Gustin et al., 2013).

135 This instrument has high temporal resolution, low limit of detection, and established  
136 quality assurance/quality control (QA/QC) protocols (Table 1). The Canadian Mercury Network  
137 (CAMNet) and the American Mercury Network (AMNet) developed best management practices  
138 for this instrument (Steffen et al., 2012; Gay et al., 2013), respectively. Co-located GEM

139 measurement can deviate by 20 to 30% (Aas, 2006; Gustin et al., 2013). Lyman et al. (2007;  
140 supplemental information) found that TGM could vary by  $7.0 \pm 5.3\%$ . There are no calibration  
141 standards for GOM; breakthrough can result in collection on the PBM filter; and collection  
142 efficiencies for GOM and PBM are uncertain (cf. Gustin and Jaffe, 2010; Huang et al., 2013;  
143 Talbot et al., 2010).

144

#### 145 2.2.2 *Lumex*

146 Lumex RA-915 and Lumex 915+ (Lumex, St. Petersburg, Russia) units measure GEM  
147 and TGM, respectively, with a reported detection limit of  $\sim 1 \text{ ng m}^{-3}$  for measurements in air. If  
148 averaged over the sampling time of the GEM measurement by the Tekran® system (5 min), a  
149 detection limit of a few tenths of  $\text{ng m}^{-3}$  can be achieved. The Lumex uses Zeeman atomic  
150 absorption spectrometry with Zeeman background correction. In this instrument, a Hg vapor  
151 lamp sits in a magnetic field and generates a 254 nm light wavelength split into 3 polarized light  
152 fields. A photodetector detects light in one field within the Hg absorption wavelength 254 nm  
153 and another lying outside of this wavelength. The signals from both fields are equal when Hg is  
154 not present (for details see Sholupov et al., 2004). The instrument can be periodically calibrated  
155 using a permeation source such as used for internal calibration of the Tekran® instruments. This  
156 is not available commercially (Dr. Franz Slemr, review ACP, March 8, 2015).

157

#### 158 2.2.3 *Gardis*

159 The Gardis Hg analyzer has two gold traps, a concentrating and analytical trap, and  
160 measures Hg using CVAAS (Institute of Physics, Lithuania). Having two gold traps might  
161 reduce some interferences such as passivation. This unit measures GEM and was developed in

162 1995 by Urba et al. (1995). In a field comparison, concentrations of GEM were similar to that  
163 measured by the Tekran® 2537 (Ebinghaus et al., 1999). This unit has had limited use and a  
164 reported detection limit of 0.5 ng m<sup>-3</sup> (Table 1).

165

166 2.2.4 University of Houston Mercury system (*UHMERC*)

167 UHMERC was designed for measuring GEM and TGM (Talbot et al., 2008). This  
168 instrument uses two Tekran® systems that are slightly modified (gold trap heated to 460 °C).  
169 The inlet to the instrument measuring GEM consists of a Teflon filter to remove fine particles  
170 (<2 µm) with a molecular sieve trap immediately after to remove GOM (Gustin et al., 2013).

171

172 2.2.5 *Detector for Oxidized Hg Species (DOHGS)*

173 The DOHGS instrument measures TGM and GEM using two Tekran® 2537 units. The  
174 difference between these measurements is interpreted as RM. The original instrument is  
175 described in Swartzendruber et al. (2009) and subsequent modifications to the system can be  
176 found in Ambrose et al. (2013), and Lyman and Jaffe (2012). The measurement of GEM requires  
177 that GOM and PBM are selectively removed from the airstream. In early versions, only GOM  
178 was removed using a KCl-coated denuder. This led to the discovery of a discrepancy between  
179 GOM collected on KCl denuders and that measured by the difference method (Swartzendruber et  
180 al., 2009). The GOM removal method was changed to quartz chips maintained at 650°C as a  
181 pyrolyzer to measure TGM, and then quartz wool (Lyman and Jaffe, 2011; Ambrose et al.,  
182 2013). More recently a cation-exchange membrane filter has been used to remove RM  
183 compounds.

184 The method detection limit for RM is  $\sim 80$  pg m<sup>-3</sup> (Ambrose et al., 2013; Table 1).  
185 Extensive testing has been conducted on the DOHGS using calibration sources of Hg<sup>0</sup>, HgBr<sub>2</sub>,  
186 and HgCl<sub>2</sub>. Ambient air RM concentrations measured by the DOHGS were higher than those  
187 measured by the Tekran® system and this instrument recovered 66% of the HgBr<sub>2</sub> spike during  
188 the Reno Atmospheric Mercury Intercomparison eXperiment (RAMIX) (Gustin et al., 2013). A  
189 major limitation of the DOHGS is the need for having two Tekran® 2537s accurately and  
190 precisely calibrated, which requires highly trained technicians. Improving the sensitivity of the  
191 underlying CVAFS systems would enable more routine operation of this instrument.

192

### 193 2.2.6 *Laser systems*

194 Two laser systems have been developed for measurement of GEM (Pierce et al., 2013  
195 Bauer et al., 2002; Bauer et al., 2010; Bauer et al., 2014). One is a cavity ring down system, and  
196 the other operates on the principle of laser-induced fluorescence. Both are calibrated using  
197 Tekran® data. These do not currently have the ability to measure GOM or PBM. If GOM and/or  
198 PBM were to be measured, they must be converted to GEM first. The cavity ring down  
199 instrument has interferences with ozone (Ashley Pierce, Ph.D. Candidate, UNR, personal  
200 communication; Pierce et al., 2013). During RAMIX these two instruments could only be  
201 operated when trained personnel were present (cf. Bauer et al., 2014). Laser systems are best  
202 applied in the lab given the current sensitivity, need for a consistent electrical supply, and large  
203 electrical power use.

204 However, during RAMIX the laser-induced fluorescence system operated by University  
205 of Miami successfully sampled on 18 days, typically for between 4 and 6 hours. The longest  
206 period of continuous sampling lasted for 26 hours. During RAMIX they sampled directly from

207 the manifold and, in addition, at the end of the campaign sampled ambient air independently,  
208 including true *in-situ* sampling on the roof of their mobile lab. They also attempted to measure  
209 RGM by pyrolyzing the sample air and measuring the difference between Hg(0) and TGM  
210 (Bauer et al, 2014; A. Hynes see open discussion this paper).

211 The University of Miami's laser system is unique in its ability to address some of the  
212 current issues regarding the atmospheric chemistry of mercury: 1) It monitors GEM *in-situ*  
213 at atmospheric pressure and composition; 2) It does not detect GOM so this does not have to be  
214 removed prior to analysis; 3) The sensitivity and temporal resolution is considerably  
215 better than any other instrument that has been deployed to measure GEM (Currently,  
216 the achievable detection sensitivity is  $15 \text{ pg m}^{-3}$  ( $5 \times 10^4 \text{ atoms cm}^{-3}$ , 2 ppq) at a  
217 sampling rate of 0.1 Hz i.e. averaging 100 shots with a 10 Hz laser system); and 4) Addition  
218 of a pyrolysis channel will allow the simultaneous measurement of total mercury and  
219 Hg(0) with high temporal resolution.

220 **2.3 Active manual samplers**

221 Here we briefly review manual sampling methods for GEM/TGM, GOM, and PBM.  
222 Manual samplers collect over a specific amount of time, and then the samples collected need to  
223 be analyzed using an alternate method. In contrast, automated samplers provide short time  
224 (seconds to minutes) resolution measurements, and do not need measurements by an alternate  
225 method.

226 *2.3.1 Mist chamber method for RM*

227 Lindberg and Stratton (1995, 1998), Lindberg et al. (2000), and Stratton et al. (2001)  
228 described development of a mist chamber for measurement of GOM (termed RGM then). The  
229 principle of operation includes pulling air at a high flow rate (15 to 20 Lpm) through a fine mist

230 aerosol made of water, NaCl, and HCl. GOM and PBM accumulate in droplets captured on a  
231 membrane. This liquid drains into a chamber, is collected, stored in vials, and analyzed using  
232 EPA Method 1631 (EPA Method 1631, 2013).

233 Sheu and Mason (2001) compared denuders, mist chambers, and a filter pack method for  
234 GOM (see SI for details). They showed GOM concentrations in Maryland could be up to 500 pg  
235  $m^{-3}$  and that GOM could be up to 30% of the TGM. Reported daytime concentrations measured  
236 by the mist chamber were significantly higher (20 to 700 pg  $m^{-3}$ ) than the denuder (20 to 70 pg  
237  $m^{-3}$ ). These data are consistent with more recent experiments demonstrating the KCl-coated  
238 denuder measurement is biased low.

239 *2.3.2 UNR Active System for GOM*

240 The UNR active system measures ambient GOM concentrations and identifies GOM  
241 compounds. It consists of a 6-port system each with two in-series Teflon filter holders. Three of  
242 the filter holders house nylon membranes and three-cation exchange membranes. Air is pulled  
243 using a vacuum pressure pump through the membranes with flow regulated by a mass flow  
244 controller at a rate of ~1 Lpm. (Huang et al., 2013). This unit is not thought to measure PBM as  
245 configured (Huang et al., 2013; 2015 this issue).

246 Cation exchange membranes are analyzed using EPA Method 1631 (EPA Method 1631,  
247 2013) to quantify GOM concentrations. Nylon membranes are thermally desorbed to determine  
248 compounds present in the air (Huang et al., 2013; this issue). This method may not collect all  
249 GOM compounds (Wright et al., 2014; Huang et al., 2014; Huang and Gustin, accepted). The  
250 nylon membrane is influenced by relative humidity (Huang et al., 2013; Huang and Gustin,  
251 under review). A summary of some advances presented in Huang and Gustin (under review)  
252 associated with this method are described in the SI. A new material is needed that is not

253 impacted by relative humidity and from which GOM can be easily thermally released. The  
254 active system is currently limited to a resolution of one-to-two weeks.

255

256 *2.3.3 Active manual systems for PBM/RM*

257 Teflon, glass-fiber, and quartz filters have been used in open faced filter packs, cascade  
258 impactors, and Micro-Orifice Uniform Deposition Impactors<sup>TM</sup> (MOUDIs) to measure  
259 atmospheric PBM concentrations (Keeler et al., 1995; Wang et al., 2013; Talbot et al., 2011;  
260 Engle et al., 2008). Although a calibrated PBM measurement could be made, for there are PBM  
261 standards, it is very difficult to separate GOM and PBM. PBM will vary depending on the  
262 chemistry of the aerosol, the atmosphere, and GOM chemistry along with physical conditions of  
263 the atmosphere, such as temperature and relative humidity. Because of this, it is currently best to  
264 measure RM. More recently RM has been collected on cation-exchange membranes using a  
265 TAPI (602) (A.Pierce, data not shown), and this measurement has shown impacts of the  
266 sampling inlet and sampling time on retention of RM. PBM measurements will collect some  
267 GOM and will be impacted by the filter material, flow rate, and inlet configuration.

268

269 **2.4 Passive samplers**

270 Passive samplers may be biotic (i.e., mosses, lichens, plant leaves) or abiotic surfaces  
271 (membranes, water). Huang et al. (2014) recently reviewed passive sampling methods for  
272 atmospheric Hg.

273 *2.4.1 Total Gaseous Mercury*

274 The method developed by Zhang et al. (2012) used an abiotic passive sampler with  
275 sulfate-impregnated carbon contained in an axial sampler. Activated carbon was investigated as a

276 sampling material for Hg by Lindberg and Turner (1977), Lindberg et al. (1979), and Lindberg  
277 (1980). Other materials that have been applied include silver wires, gold-coated plates, and gold  
278 plugs (Gustin et al., 2011; Skov et al., 2007; Huang et al. 2014). Sulfate-impregnated carbon is  
279 effective because it retains atmospheric Hg, has a high sorbtion capacity, and will not become  
280 passivated over time (cf. Huang et al., 2014). This sampler is best applied for Hg measurements  
281 across significant concentration gradients (e.g., urban-to-rural). The sampler would need to be  
282 deployed for more than 90 days at a remote site. It is not known whether it measures TGM or  
283 GEM.

284

#### 285 *2.4.2 Gaseous Oxidized Hg*

286 There are currently two types of passive samplers for GOM. These include surrogate  
287 surfaces to measure dry deposition, and a measurement of diffusive uptake as a surrogate for  
288 concentration. The most widely adopted dry deposition method uses a cation exchange  
289 membrane in a down-facing aerodynamic sampler housing (“Aerohead sampler”; Lyman et al.  
290 2007; 2009) and has been deployed in multiple studies (Castro et al., 2012; Sather et al., 2014;  
291 Sather et al., 2013; Peterson et al., 2012; Gustin et al., 2012, Wright et al., 2014b; Huang and  
292 Gustin, 2015). Although there are limitations, such as measurement of only unidirectional flux,  
293 dry deposition models also apply a similar flux. Huang and Gustin (2015) found that the  
294 surrogate surface better agreed with models when air concentrations measured by the box  
295 sampler and calibrated by the Tekran® system were adjusted by a factor of 3. The box sampler  
296 designed by Lyman et al. (2010b) provides a means for calculating concentrations based on  
297 uptake rate. Recent work suggests the box sampler has significant wall loss (80%) of GOM

298 (Huang and Gustin, 2015). Lack of calibration is a limitation for all passive samplers. The  
299 temporal resolution is coarse and samplers must be deployed for one-to-two weeks.

300

301 **2.5 Calibration methods**

302 One of the major outstanding issues is that the vast majority of GOM and PBM  
303 measurements are not calibrated (Jaffe et al., 2014). Calibration of GOM measurements has been  
304 done using manifold and chamber systems. Neither are automated or widely adopted. Coal fly  
305 ash is available as a standard for PBM, but calibrations have not been done.

306 Laboratory chambers have been developed for calibrating and testing membranes and passive  
307 samplers (Gustin et al., 2011; Lyman et al., 2007; 2010b; Skov et al., 2007).

308 The UNR manifold calibration system is designed so specific Hg compounds can be added at  
309 different concentrations as well as ozone, water vapor, and other chemical compounds. A  
310 pyrolyzer at the inlet can be used to determine concentrations of Hg being permeated (Huang et  
311 al., 2013). The 8-port glass manifold allows for collection of GOM on KCl-coated denuders and  
312 different surfaces (Huang et al., 2013). A Tekran® 2537/1130 unit at the end of the manifold is  
313 used to measure GEM and GOM concentrations. Manifold calibrations have also been performed  
314 by the University of Washington in the laboratory (Finley et al., 2013; McClure et al., 2014) and  
315 field (RAMIX; Gustin et al., 2013; Finley et al., 2013). During the RAMIX campaign,  
316 transmission efficiencies of GEM and HgBr<sub>2</sub> were 92 and 76%, respectively. Coal fly ash is  
317 available as a standard for PBM, but calibrations have not been done.

318

319

320 **3. Evolution of our understanding of the limitations of speciated Hg measurements**

321 **3.1 Are we measuring TAM, TGM, or GEM?**

322 There is debate among Hg researchers as to whether the Tekran® 2537 measures TGM  
323 versus GEM. Inlet configuration and local atmospheric chemistry will affect this measurement.  
324 Limited work in dry air with uncovered lines (i.e., exposed to sunlight) indicated that the  
325 Tekran® 2537 measures TGM (see SI). If GOM is able to pass through the inlet to the Tekran®  
326 2537 and the gold traps are not passivated, the instrument will measure TGM (Gustin et al., 2013;  
327 Temme et al., 2002). Passivation of gold surfaces can occur (Barghigiani et al., 1991; Brosset  
328 and Iverfeldt, 1989; Gustin et al., 2011; Munthe et al., 1990; Xiao et al., 1991). Passivation  
329 results in the dual traps in the Tekran® 2537 no longer being calibrated equally and loss of  
330 replication of the 5-minute measurements. Landis et al. (2002) mentioned passivation of gold  
331 traps periodically occurred right after analysis of a denuder, with recovery dropping to 50%. To  
332 measure TAM requires the use of a pyrolyzer at the inlet to the sampling line to convert GOM +  
333 PBM to GEM. Field data suggest GOM can constitute up to 25% of TGM in the tropics and mid-  
334 latitudes (Brunke et al., 2010), in Nevada, Florida, and Maryland (see discussion above and  
335 below), and up to 100% during depletion events in the Arctic (Steffen et al., 2015).

336

337 **3.2 PBM measurements and potential artifacts**

338 PBM measurements have received relatively little systematic study. The Tekran® system  
339 is currently the most widely used configuration for measuring PBM. Other sampling methods  
340 tested include filter-based methods (Rutter et al., 2008; Talbot et al., 2011; Malcom and Keeler,  
341 2007; Kim et al., 2012). The sign and magnitude of the PBM bias is presently unclear. Both high  
342 and low biases have been reported for the Tekran® PBM measurement (Talbot 2011; Rutter  
343 2008; Malcolm 2007; Gustin et al., 2013).

344 The particle size distribution of PBM is spatially heterogeneous and can include both fine  
345 and coarse fractions (Kim et al., 2012; Keeler et al., 1995; Keeler and Malcom, 2007; Engle et  
346 al., 2008). The standard inlet on the Tekran® 2537/1130/1135 excludes particles larger than 2.5  
347  $\mu\text{m}$  (depending on the flow rate; Lyman et al, 2010) in diameter to prevent large particles from  
348 depositing on the KCl-coated denuder. Thus in coastal/marine, agricultural, or industrial settings  
349 with high concentrations of large particles, reported PBM concentrations represent a lower  
350 bound (Malcolm and Keeler, 2007; Kim et al., 2012; Poissant et al., 2005). Surrogate surfaces  
351 with cation exchange membranes may collect small aerosol fractions (Lyman et al., 2007).

352 Temperature and atmospheric composition potentially impact PBM measurements. The  
353 Tekran® 1135 particulate module is maintained at 50°C to prevent condensation of water vapor.  
354 Based on filter experiments compared with Tekran® PBM, Rutter et al. (2008) suggested there is  
355 evaporative loss of PBM. Thermal desorption profiles using nylon membranes showed that  
356 Hg(II) compounds are emitted at temperatures ranging from 50 to 200°C (Figure 2), depending  
357 on charges on the collection surface and the polarizability of the different Hg compounds (Huang  
358 et al., 2013). Malcolm and Keeler (2007) observed less PBM collected on quartz filters for 12  
359 versus 4 h, and suggested a negative sampling artifact associated with relative humidity or  
360 reaction with gases in the air such as O<sub>3</sub>.

361 Breakthrough of GOM and/or inadvertent retention of GOM on the PBM collection  
362 surface can bias PBM measurements high. In principal, the Tekran® 2537/1130/1135 removes  
363 GOM on the KCl-coated annual denuder and then PBM is collected downstream. Field data has  
364 shown that GOM compounds not collected by the KCl-coated denuder can be captured by the  
365 particulate unit (Gustin et al., 2013). Quartz fiber filters used to collect PBM may also collect  
366 GOM (Rutter et al., 2007; See SI for detailed example). Lyman et al. (2007) compared calculated

367 dry deposition fluxes associated with coated (KCl) and uncoated quartz fiber filters against data  
368 collected using cation-exchange membranes, both yielded significantly lower deposition fluxes.  
369 This agrees with the lack of capture and retention by the KCl-coated denuder. GOM  
370 breakthrough may not occur in all cases. For example, if there are temperature drops within the  
371 instrument, then GOM will deposit to the walls. The authors conclude it is presently more robust  
372 to interpret RM rather than PBM and GOM data separately until a new denuder coating is tested  
373 and brought into use.

374

375 **3.3 GOM: Biases, interferences, and shedding light on the spatiotemporal variability of**  
376 **GOM compounds in air**

377 Based on laboratory and field studies, concentrations of GOM collected on the nylon and  
378 cation exchange membranes are higher than those collected by the Tekran® system by 60-  
379 1000% (Huang et al., 2014; Huang and Gustin, this issue 2015; Huang and Gustin, in review).  
380 Laboratory and field experiments have demonstrated the collection efficiency of KCl-coated  
381 denuders varies with environmental conditions (ozone, relative humidity) and Hg(II) compounds  
382 present in air. Below we discuss recent laboratory experiments and field studies that have shaped  
383 our understanding of the limitations of GOM measurement methods.

384

385 *3.3.1 Ozone and relative humidity interferences*

386 Laboratory experiments have confirmed ozone ( $O_3$ ) interferences for KCl-coated  
387 denuders and relative humidity (RH) interferences for both denuders and nylon membranes  
388 (Lyman et al., 2010a; McClure et al., 2014; Huang and Gustin, 2015). Lyman et al. (2010a)  
389 found the collection efficiency of  $HgCl_2$  loaded on a KCl denuder was reduced by 3 to 37%

390 when O<sub>3</sub> concentrations were 6 to 100 ppbv. Lyman et al. (2010a Open Discussion) proposed  
391 reduction was occurring on the denuder wall:



393 Their results also indicated less GOM was recovered as O<sub>3</sub> exposure time increased (10 to 26%  
394 removed from loaded denuders for 2.5 minutes, and 29 to 55% for 30 minutes at 30 ppbv).

395 In experiments similar to those performed for O<sub>3</sub>, McClure et al (2014) found RH had a  
396 similar effect on HgBr<sub>2</sub> loaded on KCl-coated denuders. Huang and Gustin (2015) permeated  
397 HgBr<sub>2</sub> and water vapor into a Tekran® 2357/1130 system in ambient air and found collection  
398 efficiencies dropped during the spikes of RH, and the denuder became passivated over time.

399

400 *3.2.2 Evidence for spatial and temporal variability of RM concentrations in air*

401 Here we use comparisons of data collected with the Tekran® system with alternative  
402 systems to better understand atmospheric Hg concentrations. This includes data collected as part  
403 of a large study in Florida (Peterson et al., 2012; Gustin et al., 2012), the RAMIX field campaign  
404 (Gustin et al., 2013), recent comparison of KCl-coated denuder data with the UNR active system  
405 (Huang et al., 2013; 2015 this issue), and laboratory testing (Huang et al., 2013; Huang and  
406 Gustin, 2015 under review). For a historical review of additional literature see the supplemental  
407 information in Gustin et al., 2013, Huang et al., 2014, and SI this paper.

408 Peterson et al. (2012) compared passive samplers and Tekran® data from three sites in  
409 Florida. The region has high Hg wet deposition, but low GOM concentrations (on average 2-8 pg  
410 m<sup>-3</sup> as measured by the Tekran® system). In general, the Aerohead derived data showed higher  
411 deposition for GOM than that calculated using KCl-coated denuder measurements and a dry  
412 deposition model. Based on passive sampler uptake and calculated deposition velocities,

413 Peterson et al. (2012) suggested the difference could be explained by the presence of different  
414 GOM compounds in the air (see SI for additional detail). Examining the data across all seasons  
415 using 3 Hg measurement methods, criteria pollutants, and meteorology, Gustin et al. (2012)  
416 concluded there were different GOM compounds in air that were derived from different primary  
417 sources, and sources producing different oxidants.

418 The RAMIX experiment further demonstrated the KCl-denuder measurements were  
419 biased low through spikes of GOM ( $\text{HgBr}_2$ ) into a manifold. The experiment also indicated RH  
420 caused the denuders to become passivated over time (Gustin et al., 2013). Spike recoveries of  
421  $\text{HgBr}_2$  by KCl-coated denuders were 2-to-5 times lower than that measured by the DOHGS, with  
422 mean values for spikes ranging from 17 to 23% recovery. Replicate nylon membranes collected  
423 30 to 50% more RM than the Tekran® system in ambient air. These all point to the lack of  
424 collection efficiency of the denuder measurement. Similar results were found in laboratory tests  
425 described below. For a concise summary of the results of the RAMIX DOHGS versus Tekran®  
426 data, and an explanation for a component of the atmospheric chemistry occurring see the SI.

427 Figure 1 and Table 2 show the correlation between specific GOM compounds  
428 concentrations measured by the nylon and cation exchange membranes versus the KCl-coated  
429 denuder in the Tekran® system (see Huang et al. (2013) for detail on the experimental setup).  
430 These data demonstrate different compounds have different collection efficiencies by the  
431 denuder. Figure 1 shows the nylon membrane has equal efficiency for all Hg(II) compounds  
432 tested, and the cation exchange membrane quantitatively collects the Hg(II) compounds  
433 permeated. The collection efficiency of the cation exchange membrane relative to the KCl-  
434 coated denuder in a Tekran® 1130 is  $\text{HgBr}_2$  (1.6)> $\text{HgSO}_4$  (2.3)= $\text{HgCl}_2$  (2.4)> $\text{HgO}$  (3.7)  
435 > $\text{Hg}(\text{NO}_3)_2$  (12.6).

436 Huang et al. (2013) compared field data collected using the Tekran® system and the  
437 UNR active system. Cation-exchange membranes measured concentrations were 1.1-to-3.7 times  
438 greater than the nylon membranes, and 2-to-6 times greater than Tekran® RM values.  
439 Substantial spatial and temporal variability in the difference between the cation-exchange  
440 membrane and Tekran® RM values were observed. Thermal desorption profiles from the nylon  
441 membranes indicate this is explained by variability in the Hg(II) compounds present in air  
442 (Huang et al., 2013). Huang et al. (2015; this issue) report thermal desorption profiles from the  
443 marine boundary layer in Florida. The cation exchange membranes reported higher  
444 concentrations than the Tekran® RM measured, and the nylon membranes had different  
445 desorption profiles that could be attributed to specific sources.

446 Laboratory and field experiments indicate that the collection efficiency of the KCl-coated  
447 denuder varies depending on environmental conditions (ozone, relative humidity) and Hg(II)  
448 compounds present in air. As we are learning about fundamental limitations of current  
449 measurements and testing new methods, evidence is coalescing to demonstrate that GOM  
450 compounds in the air vary seasonally and spatially.

451

#### 452 **4. Case study demonstrating how we can use past measurements to move forward**

453 In light of the new information about interferences affecting GOM measurements, we  
454 may begin to go back and re-examine features of past data that previously could not be  
455 explained. Here we explore Weiss-Penzias et al. (2003) as a case study. They measured GEM,  
456 GOM, and PBM at Cheeka Peak Observatory, Washington, US, in the marine boundary layer  
457 and found “air of continental origin containing anthropogenic pollutants contained on average  
458 5.3% lower GEM levels as compared with the marine boundary”. GOM and PBM concentrations

459 in continental air were very low, 0 – 20 pg m<sup>-3</sup> and 1-4 pg m<sup>-3</sup>, respectively. At the time, the  
460 results were “difficult to reconcile”. Now we see that the change in GEM concentration during  
461 local anthropogenic pollution events relative to the mean of monthly marine air (-60 to -270 pg  
462 m<sup>-3</sup>) in Weiss-Penzias et al. (2003) are similar to the disparity in concentrations measured during  
463 RAMIX between the DOHGS and Tekran® RM measurement. This observation indicates that  
464 loss of GEM in air can be used to estimate GOM concentrations.

465 Retrospectively, we suggest the observed differences between the two air masses reported  
466 can be explained by differences in the mix of oxidants and the resultant Hg(II) compounds  
467 formed. GOM and PBM were likely low due to lack of collection efficiency, interferences with  
468 O<sub>3</sub>, and loss in the sampling line (see SI for details of sampling set up). Significantly lower GEM  
469 concentrations in the continental air are indicative of greater oxidation, which is supported by  
470 decreases in GEM concentrations coincident with ozone increases. Eastern Washington is  
471 covered by forests, which generate volatile organic compounds that could contribute to ozone  
472 and GOM formation. The marine air masses likely contained HgBr<sub>2</sub> or HgCl<sub>2</sub> and the continental  
473 air Hg-O, Hg-S, Hg-N compounds associated with industry, agriculture, and mobile sources. The  
474 capture efficiency of HgBr<sub>2</sub> and HgCl<sub>2</sub> is greater than for O, S, and N compounds (Figure 1;  
475 Table 2).

476

477 **5. Advancing understanding using Hg measurements and models**

478 Here we discuss several key scientific advancements that have come from comparing  
479 models with speciated measurements, as well as the major questions left open by these studies.  
480 The number of atmospheric models capable of simulating speciated Hg has multiplied over the  
481 last decade (Table 3). Detailed discussion on model/measurement comparisons of RM can be

482 found in Kos et al. (2013). Limitations and uncertainties of the models themselves have been  
483 written about at length in the original research articles and in model intercomparisons (Bullock et  
484 al., 2008; Pongprueksa et al., 2008; Lin et al., 2006). Fully acknowledging current limitations,  
485 there have still been huge strides made in our scientific understanding of the processes  
486 controlling GEM, GOM, and PBM cycling in the atmosphere including: marine boundary layer  
487 cycling, plume chemistry, source-receptor relationships, gas-particle partitioning, and vertical  
488 distribution.

489 Our understanding of speciated Hg cycling in the marine boundary layer (MBL) is one  
490 example of Hg science advancing as a result of using measurements and models in combination. GOM  
491 in the MBL has a diurnal pattern characterized by a midday peak and is depleted through  
492 deposition at night (Laurier & Mason, 2007; Laurier et al., 2003; Sprovieri et al., 2003). The use  
493 of observations and models together determined that the MBL has bromine photochemistry, and  
494 was not affected by the hydroxyl (OH) radical. This drives the midday photochemical peak in  
495 GOM concentrations in the MBL and that scavenging by sea-salt was driving rapid deposition at  
496 night (Holmes et al., 2009; Selin et al., 2007; Obrist et al., 2010; Hedgecock and Pirrone, 2001,  
497 2004; Hedgecock et al., 2003; Jaffe et al., 2005; Laurier and Masson 2007; Laurier et al., 2003;  
498 Sprovieri et al., 2003) .

499 Model-observation comparisons consistently suggest models overestimate GOM surface  
500 concentrations, sometimes by as much as an order of magnitude (Amos et al., 2012; Zhang et al.,  
501 2012; Kos et al., 2013; Holloway et al., 2012; Bieser et al., 2014). The measurement-model  
502 mismatch is now understood as being partly explained by a low sampling bias (see Section 3),  
503 but this alone cannot reconcile the discrepancy. Reduction of GOM to GEM in coal-fired power  
504 plant plumes (Edgerton et al., 2006; Lohman et al., 2006) has been invoked as a possible

505 explanation (Amos et al., 2012; Zhang et al., 2012; Kos et al., 2013; Holloway et al., 2012;  
506 Vijayaraghavan et al., 2008). The mechanism for in-plume reduction (IPR) remains speculative,  
507 hindering inference about how in-plume reduction may vary with coal type, control technology,  
508 or atmospheric composition. Results from recent field and laboratory data have been mixed,  
509 providing evidence for and against IPR (Tong et al., 2014; Landis et al., 2014) (Deeds et al.,  
510 2013). As IPR is explored, it has become apparent the speciation of anthropogenic emission  
511 inventories may need to be revisited in order to reconcile the model-measurement RM mismatch  
512 (Wang et al., 2014; Bieser et al., 2014). Getting a better handle on IPR and emission speciation  
513 has important implications for the efficacy of domestic regulation such as the US EPA Mercury  
514 Air Toxics Standard and for potentially attributing trends in Hg wet deposition over the US  
515 (Zhang et al., 2013).

516 Derived source-receptor relationships will also be sensitive to uncertainties in IPR and  
517 emission speciation. On the whole Hg models better simulate wet deposition fluxes than surface  
518 GOM concentrations, contributing to the relatively high degree of consensus among source-  
519 receptor studies. A comparison of source-receptor studies found models agreed within 10% in  
520 terms of the attribution of total wet Hg deposition to a given continental region (e.g., Europe,  
521 Asia) (AMAP/UNEP, 2013; Travnikov et al., 2010). Several source-receptor studies have  
522 concluded domestic US emissions contribute ~20% to total Hg deposition over the contiguous  
523 US (Selin and Jacob, 2008; Corbitt et al., 2011). Zhang et al. (2012) found that including IPR in  
524 a model decreased the domestic contribution to wet deposition over the United States from 22 to  
525 10%.

526 An additional area of measurement-model study has been gas-particle partitioning of  
527 GOM and PBM. Understanding gas-particle partitioning is important because gases and particles

528 are removed from the atmosphere by different physical processes. There is strong observational  
529 and laboratory evidence that gas-particle partitioning between GOM and PBM is driven by air  
530 temperature and aerosol concentrations (Rutter and Schauer, 2007a and b; Steffen et al., 2014)  
531 (Rutter et al., 2008; Amos et al., 2012; Chen et al., 2014). Implementing temperature-dependent  
532 gas-particle partitioning in a global model increased simulated annual Hg deposition at higher  
533 latitudes (Amos et al., 2012). Aircraft observations suggest gas-particle partitioning also plays a  
534 major role in influencing the vertical profile of Hg, especially in the upper troposphere/lower  
535 stratosphere (UTLS) (Swartzendruber et al., 2009; Lyman and Jaffe, 2012; Murphy et al., 2006).  
536 Current gas-particle partitioning relationships are derived from surface data. PBM measurements  
537 from the summit of Mt. Bachelor suggest these relationships do not capture PBM dynamics aloft  
538 (Timonen et al., 2013). Effects of aerosol composition (Rutter and Schauer, 2007b), relative  
539 humidity, or even repartitioning of RM within the Tekran® (see section 3.3) could potentially  
540 contribute to this deficiency.

541 Oxidation also plays a central, but poorly characterized, role in Hg cycling at the upper  
542 troposphere/lower stratosphere boundary. Comparisons against vertical aircraft profiles of TGM  
543 consistently suggest there is too little oxidation in models in the lower stratosphere (Zhang et al.,  
544 2012; Holmes et al., 2010; Hannah M. Horowitz, PhD Candidate, Harvard University,  
545 Department of Earth & Planetary Sciences personal communication). Observations show that  
546 total Hg is depleted in the lower stratosphere (Holmes et al., 2010; Lyman and Jaffe, 2012; Slemr  
547 et al., 2014), which is thought to be the result of rapid oxidation of Hg(0) to Hg(II), partitioning  
548 of Hg(II) to sulfate aerosol, and subsequent sedimentation of PBM (Lyman and Jaffe, 2012).  
549 Aircraft measurements over Washington and Tennessee, US, found summertime GOM peaks  
550 between 2-4 km (Swartzendruber et al., 2009; Brooks et al., 2014). Modeled GOM vertical

551 profiles over the US have a less pronounced peak and generally place it higher (4-6 km) (Bullock  
552 et al., 2008). Correctly modeling the vertical distribution of Hg, particularly GOM and PBM, is  
553 essential for simulating deposition and hence Hg loading to surface ecosystems.

554 Chemistry remains the greatest uncertainty in Hg models. Improving the reliability of  
555 GOM and PBM measurements can help determine the mechanism(s) at play. There is still a  
556 general lack of rate coefficients and corresponding step-by-step reaction mechanisms available.  
557 The estimated tropospheric lifetime of RM against deposition and reduction is 40 days (Holmes  
558 et al., 2010), but the reduction pathway is extremely uncertain (Subir et al., 2011; Pongprueska et  
559 al., 2008), and the burden of RM in the free troposphere is uncertain by at least a factor of two  
560 (Selin et al., 2008; De Simone et al., 2014). Improving our knowledge of the reduction and  
561 oxidation rates in the atmosphere will allow models to better capture the vertical distribution of  
562 Hg, and in turn better simulate Hg deposition. The recent AMAP/UNEP (2013) assessment  
563 identified this as the highest priority for Hg models due to the importance in the Hg exposure  
564 pathway.

565 A persistent issue is the ambiguity in comparing modeled Hg(II) compounds to GOM and  
566 PBM, which are operationally defined. Models either have a lumped Hg(II) tracer or explicitly  
567 resolve individual Hg(II) compounds (Table 3). Since different Hg(II) compounds have different  
568 collection efficiencies by the KCl-denuder (Figure 1), this further confounding how to best  
569 construct a GOM-like model quantity to compare against observations. An active dialogue  
570 between researchers and modelers is encouraged as the community moves forward, so modelers  
571 may implement Hg tracers that emulate the Hg compounds measured.

572 The analytical uncertainties associated with GOM and PBM measurements place  
573 limitations on model development. Presently the absolute bias in GOM and PBM concentrations

574 is not entirely known or quantified (Jaffe et al., 2014). Observations serve a vitally important  
575 function for models by anchoring them to reality, and reconciliation of model-measurement  
576 mismatches can spur important advances in our understanding of Hg cycling. This process has  
577 become impeded by recent revelations that GOM and PBM measurements are affected by biases  
578 and interferences that vary in space and time. From a modeling perspective, the magnitude of the  
579 sampling bias does not matter as long as there is a robust, quantitative correction factor to apply  
580 to affected measurements.

581       Recent papers have used a 3-fold correction factor to adjust the GOM measurements  
582 made in the Western United States and Florida (cf. Huang and Gustin, 2015; Huang et al. this  
583 issue). Use of this correction factor is based on the discrepancy between denuder measurements  
584 in the field and cation exchange membranes collected using the UNR active system. These field  
585 observations were collected in dry and humid conditions, and at ozone concentrations typically  
586 observed in the atmosphere. Others could use this same correction factor. Additional  
587 consideration could be based on the relative humidity and ozone concentrations, and the potential  
588 GOM compounds in the air. The correction factor worked relatively well in a dry and humid  
589 location (cf. Huang and Gustin 2015 and this issue).

590       Huang and Gustin (2015) examined the relationship between RH and GOM capture by  
591 the denuder. They found at RH of 21 to 62%:

592        $RH = 0.63 \text{ GOM loss\%} + 18.1, r^2 = 0.49, p\text{-value} < 0.01.$  Equation 2.

593       Similarly Lyman et al. (2010a) found a decrease in GOM with ozone exposure. Both studies  
594 found that passivation occurs over time. However, Huang and Gustin (2015) found a greater  
595 impact of relative humidity. The case study exemplifies how we can use the loss of GEM as a  
596 means of understanding the amount of GOM present or produced in air.

597 **6. Outstanding issues**

598 Mercury is present in the atmosphere at  $\text{pg m}^{-3}$  to  $\text{ng m}^{-3}$ , and the capability to measure it  
599 is a substantial analytical accomplishment. High quality, ongoing measurements of atmospheric  
600 Hg will be key in evaluating the environmental benefit of regulation on behalf of the Convention.

601 Here we reviewed the current state of the science for measuring and modeling  
602 atmospheric Hg concentrations. Recent laboratory and field investigations have shown numerous  
603 artifacts and environmental interferences can affect measurement methods. Some environments  
604 such as those with low humidity and ozone may be less susceptible to sampling interferences  
605 than others. In light of new information about the limitations of sampling methods, we may  
606 revisit and better explain certain features of previous data sets and measurement-model  
607 comparison. Moving forward, data will need to be interpreted within this new paradigm.

608 Fundamental research is needed on measurement methods and the atmospheric chemistry  
609 of Hg. This will better address the needs of the Convention and also help support model  
610 development. Identifying the chemical compounds of RM in the atmosphere is a top priority.  
611 Understanding the final oxidation products are key for resolving questions regarding Hg  
612 chemistry. Knowing the dominant compounds would help with the design of measurement  
613 methods and determination of deposition velocities.

614 Thermal desorption shows promise and the concept has already been proven for field  
615 measurements taken in Nevada and Florida. Mass spectrometry may be a way to verify  
616 compounds.

617 We need to obtain agreement between several methods for understanding the chemical  
618 forms and compounds in the air. Only through comparison of multiple calibrated measurements  
619 can results be determined to be accurate.

620        With an understanding of the different chemical compounds in the air, development of a  
621    standard, field-deployable calibration system is needed. This system should provide spikes into  
622    ambient air and allow for studying sampling efficiencies and artifacts associated with ambient  
623    air. Lack of calibration is currently a major shortcoming.

624        Data collected using the UNR Active System can be compared to KCl-coated denuder  
625    measurements in different areas and used for understanding the GOM concentrations and  
626    chemistry for different areas.

627        Improvements to the Tekran® 2537/1130/1135 system are needed. A pyrolyzer should be  
628    used at the inlet of the 2537 if the goal is to measure TAM. The way the Tekran® 1130/1135  
629    system is configured to capture GOM first and then PBM is the best method to measure these  
630    two compounds. However, given the difficulty of separating GOM from PBM, we recommend  
631    interpreting the sum of RM instead of PBM alone until separation is improved.

632        The depletion of GEM measured in air can be used as a surrogate for estimating RM  
633    concentrations in past measurements. We present a case study which demonstrates this can be  
634    done successfully for marine boundary layer and continental air.

635        A measurement system that collects GOM on a denuder material that has been  
636    demonstrated to work for all compounds of GOM, and separate measurement on a filter using a  
637    cation-exchange membrane could be used for measurement of GOM and RM. Then the PBM  
638    could be determined by difference. Due to negative artifacts during long sampling times  
639    measurements should be done for < 24 h.

640        A new passive sampler design is needed that quantitatively determines concentrations  
641    and is calibrated. Use of a computational fluid dynamics model to help design the sampler could

642 be one successful way forward. Passive samplers and surrogate surfaces have longer time  
643 resolution (1 day to 1 week), but are relatively inexpensive and easy to operate and could provide  
644 an alternative measure of GOM concentrations and dry deposition fluxes in large-scale sampling  
645 networks once the above issues are resolved.

646 Since atmospheric GEM concentrations are decreasing in some locations, and  
647 atmospheric oxidants are increasing then GOM concentrations must be increasing. This  
648 hypothesis needs to be further explored, and could have significant implications for the Minimata  
649 Convention.

650

651

## 652 **Acknowledgements**

653 This manuscript was initiated by discussions at the “Data Collection, Analysis and  
654 Application of Speciated Atmospheric Mercury” Workshop coordinated by Leiming Zhang and  
655 held 29 July 2014 in San Francisco, California. Work at UNR was supported by the National  
656 Science Foundation (Awards: 0850545, 0917934, 1102336, 1326074), the Electric Power  
657 Research Institute, and The Southern Company. We thank Drs. Dan Jaffe and Steve Lindberg for  
658 comments on an early version of this manuscript. We thank Dr. Franz Slemr for his extensive  
659 review and constructive comments, an anonymous reviewer for his/her comments; and Tony  
660 Hynes for providing information on his instrument that has now been included in the paper.  
661 M.S.G. thanks all the undergraduate students who analyze samples in the lab, for this work could  
662 not have been done without their conscientious efforts and Michael Gustin for his continued  
663 support.

664

665 **References cited.**  
666  
667 Aas, W (ed.): Data quality 2004, quality assurance, and field comparisons, C587 EMEP/CCC-Report  
668 4/2006, NILU, Kjeller, Norway 2006.  
669

670 AMAP/UNEP: Technical Background Report for the Global Mercury Assessment 2013., Arctic Monitoring  
671 and Assessment Program, Oslo, Norway / UNEP Chemicals Branch, Geneva, Switzerland, vi + 263 pp,  
672 <http://www.unep.org/PDF/PressReleases/GlobalMercuryAssessment2013.pdf> 2013.  
673 Ambrose, J.L., Lyman, S.N., Huang, J., Gustin, M., Jaffe, D.A.: Fast Time Resolution Oxidized  
674 Mercury Measurements with the UW Detector for Oxidized Hg Species (DOHGS) during the Reno  
675 Atmospheric Mercury Intercomparison Experiment, Environ. Sci. Technol., 2013.  
676  
677 Amos, H. M., Jacob, D. J., Holmes, C. D., Fisher, J. A., Wang, Q., Yantosca, R. M., Corbitt, E. S., Galarneau,  
678 E., Rutter, A. P., Gustin, M. S., Steffen, A., Schauer, J. J., Graydon, J. A., St Louis, V. L., Talbot, R. W.,  
679 Edgerton, E. S., Zhang, Y., and Sunderland, E. M.: Gas-particle partitioning of atmospheric Hg(II) and its  
680 effect on global mercury deposition, Atmos. Chem. Phys., 12, 591-603, doi:10.5194/acp-12-591-2012,  
681 2012.  
682

683 Bargigiani, C., Ristori, T., Cortopassi, M.: Air mercury measurement and interference of atmospheric  
684 contaminants with gold traps, Environ. Technol., 12, 935-941, 1991.  
685  
686 Bauer, D., Everhart, S., Remeika, J., Tatum Ernest, C., Hynes, A. J.: Deployment  
687 of a Sequential Two-Photon Laser Induced Fluorescence Sensor for the Detection  
688 of Gaseous Elemental Mercury at Ambient Levels: Fast, Specific, Ultrasensitive Detection  
689 with Parts-Per-Quadrillion Sensitivity, Atmos. Meas. Tech., 7, 4251-4265, 2014  
690 doi:10.5194/amt-7-4251-2014.  
691  
692  
693 Bauer, D., Campuzano-Jost, P., Hynes, A.J.: Rapid, ultra-sensitive detection of gas phase elemental  
694 mercury under atmospheric conditions using sequential two-photon laser induced fluorescence,  
695 Environ. Monit., 4, 339-343, 2002.  
696  
697 Bauer, D., Swartzendruber, P.C., Hynes, A.J.: Deployment of a compact sequential 2 Photon LIF detection  
698 system for gaseous elemental mercury at ambient levels, Geochimica Et Cosmochimica Acta, 74, A60-  
699 A60, 2010.  
700  
701 Bieser, J., De Simone, F., Gencarelli, C., Geyer, B., Hedgecock, I., Matthias, V., Travnikov, O., and Weigelt,  
702 A.: A diagnostic evaluation of modeled mercury wet depositions in Europe using atmospheric speciated  
703 high-resolution observations, Environ. Sci. Pollut. Res., 21, 9995-10012, doi: 10.1007/s11356-014-2863-  
704 2, 2014.  
705 Brosset, C., Iverfeldt, A.: Interaction of solid gold surfaces with mercury in ambient air, Water Air Soil  
706 Poll., 43, 147-168, 1989.  
707

708 Brooks, S., Ren, X., Cohen, M., Luke, W., Kelley, P., Artz, R., Hynes, A., Landing, W., and Martos, B.:  
709 Airborne Vertical Profiling of Mercury Speciation near Tullahoma, TN, USA, *Atmosphere*, 5, 557-574,  
710 2014.

711

712 Brunke, E.-G., Labuschagne, C., Ebinghaus, R., Kock, H. H., Slemr, F.: Gaseous elemental mercury  
713 depletion events observed at Cape Point during 2007–2008, : *Atmospheric Chemistry and Physics*, 10,  
714 1121-1131, 2010.

715

716 Bullock, O. R., Atkinson, D., Braverman, T., Civerolo, K., Dastoor, A., Davignon, D., Ku, J. Y., Lohman, K.,  
717 Myers, T. C., Park, R. J., Seigneur, C., Selin, N. E., Sistla, G., and Vijayaraghavan, K.: The North American  
718 Mercury Model Intercomparison Study (NAMMIS): Study description and model-to-model comparisons,  
719 *J. Geophys. Res.-Atmos.*, 113, 17, doi: 10.1029/2008jd009803, 2008.

720 Castro, M.S., Moore, C., Sherwell, J., Brooks, S.B.: Dry deposition of gaseous oxidized mercury in  
721 Western Maryland, *Sci. Total Environ.*, 417, 232-240, 2012.

722

723 Cole, A.S., Steffen, A.: Trends in long-term gaseous mercury observations in the Arctic and effects of  
724 temperature and other atmospheric conditions, *Atmos. Chem. Phys.*, 10, 4661-4672, 2010.

725

726 Cole, A.S., Steffen, A., Eckley, C.S., Narayan, J., Pilote, M., Tordon, R., Graydon, J.A., St Louis, V.L., Xu, X.,  
727 Branfireun, B.A.: A Survey of Mercury in Air and Precipitation across Canada: Patterns and Trends,  
728 *Atmosphere*, 5(3), 635-668, 2014.

729

730 Corbitt, E. S., Jacob, D. J., Holmes, C. D., Streets, D. G., and Sunderland, E. M.: Global Source–Receptor  
731 Relationships for Mercury Deposition Under Present-Day and 2050 Emissions Scenarios, *Environ. Sci.*  
732 *Technol.*, 45, 10477-10484, doi: 10.1021/es202496y, 2011.

733 Deeds, D.A., Banic, C.M., Lu, J., Daggupaty, S.: Mercury speciation in a coal-fired power plant plume: An  
734 aircraft-based study of emissions from the 3640 MW Nanticoke Generating Station, Ontario, Canada,  
735 *Geophys. Research-Atmos.*, 118, 4919-4935, 2013.

736

737 Dibble, T.S., Zelie, M.J., Mao, H.: Thermodynamics of reactions of ClHg and BrHg radicals with  
738 atmospherically abundant free radicals, *Atmos. Chem. Phys.*, 12, 10271-10279, 2012.

739

740 Ebinghaus, R., Jennings, S.G., Schroeder, W.H., Berg, T., Donaghy, T., Guentzel, J., et al.: International  
741 field intercomparison measurements of atmospheric mercury species at Mace Head, Ireland, *Atmos.*  
742 *Environ.*, 33, 3063-3073, 1999.

743

744 Engle, M.A., Tate, M.T., Krabbenhoft, D.P., Kolker, A., Olson, M.L., Edgerton, E.S., et al.: Characterization  
745 and cycling of atmospheric mercury along the central US Gulf Coast, *Appl. Geochem.*, 23, 419-437, 2008.

746

747 Engstrom, D.R., Fitzgerald, W.F., Cooke, C.A., Lamborg, C.H., Drevnick, P.E., Swain, E.B., et al.:  
748 Atmospheric Hg Emissions from Preindustrial Gold and Silver Extraction in the Americas: A Reevaluation  
749 from Lake-Sediment Archives, *Environ. Sci. Technol.*, 48, 6533-6543, 2014.

750

751 EPA Method 1631: <http://water.epa.gov/scitech/methods/cwa/metals/mercury/index.cfm> , accessed:  
752 December 27, 2014.

753

754 Finley, B.D., Jaffe, D.A., Call, K., Lyman, S., Gustin, M.S., Peterson, C., et al.: Development, Testing, And  
755 Deployment of an Air Sampling Manifold for Spiking Elemental and Oxidized Mercury During the Reno  
756 Atmospheric Mercury Intercomparison Experiment (RAMIX), *Environ. Sci. Technol.*, 47, 7277-7284, 2013.  
757

758 Deeds, D.A., Banic, C.M., Lu, J., Daggupaty, S.: Mercury speciation in a coal-fired power plant plume: An  
759 aircraft-based study of emissions from the 3640 MW Nanticoke Generating Station, Ontario, Canada,  
760 *Geophys. Research-Atmos.*, 118, 4919-4935, 2013.  
761

762 Gay, D.A., Schmeltz, D., Prestbo, E., Olson, M., Sharac, T., Tordon, R.: The Atmospheric Mercury  
763 Network: measurement and initial examination of an ongoing atmospheric mercury record across North  
764 America, *Atmos. Chem. Phys.*, 13, 11339-11349, 2013.  
765

766 Gustin, M., Jaffe, D.: Reducing the Uncertainty in Measurement and Understanding of Mercury in the  
767 Atmosphere, *Environ. Sci. Technol.*, 44, 2222-2227, 2010.  
768

769 Gustin, M. S. Exchange of Mercury between the Atmosphere and Terrestrial Ecosystems, in:  
770 Environmental Chemistry and Toxicology of Mercury, Liu, G., Cai, Y., O'driscoll, N., John Wiley and Sons,  
771 Hoboken, New Jersey, 423-452, 2011.  
772

773 Gustin, M.S., Huang, J., Miller, M.B., Peterson, C., Jaffe, D.A., Ambrose, J., et al.: Do We Understand  
774 What the Mercury Speciation Instruments Are Actually Measuring? Results of RAMIX, *Environ. Sci.*  
775 *Technol.*, 47(13), 7295-7306, 2013.  
776

777 Gustin, M.S., Lindberg, S.E.: Assessing the contribution of natural sources to the global mercury cycle:  
778 The importance of intercomparing dynamic flux measurements, *Fresen. J. Anal. Chem.*, 366, 417-422,  
779 2000.  
780

781 Gustin, M.S., Lyman, S.N., Kilner, P., Prestbo, E.: Development of a passive sampler for gaseous mercury,  
782 *Atmos. Environ.*, 45, 5805-5812, 2011.  
783

784 Gustin, M.S., Weiss-Penzias, P.S., Peterson, C.: Investigating sources of gaseous oxidized mercury in dry  
785 deposition at three sites across Florida, USA, *Atmos. Chem. Phys.*, 12, 9201-9219, 2012.  
786

787 Hedgecock, I. M., and Pirrone, N.: Mercury and photochemistry in the marine boundary layer-modeling  
788 studies suggest the in situ production of reactive gas phase mercury, *Atmos. Environ.*, 35, 3055-3062,  
789 doi: 10.1016/s1352-2310(01)00109-1, 2001.  
790

791 Hedgecock, I. M., Pirrone, N., Sprovieri, F., and Pesenti, E.: Reactive gaseous mercury in the marine  
792 boundary layer: modelling and experimental evidence of its formation in the Mediterranean region,  
793 *Atmos. Environ.*, 37, S41-S49, doi: 10.1016/s1352-2310(03)00236-x, 2003.  
794

795 Hedgecock, I. M., and Pirrone, N.: Chasing quicksilver: Modeling the atmospheric lifetime of Hg-(g)(0) in  
796 the marine boundary layer at various latitudes, *Environ. Sci. Technol.*, 38, 69-76, doi:  
797 10.1021/es034623z, 2004.  
798

799 Holloway, T., Voigt, C., Morton, J., Spak, S. N., Rutter, A. P., and Schauer, J. J.: An assessment of  
800 atmospheric mercury in the Community Multiscale Air Quality (CMAQ) model at an urban site and a

801 rural site in the Great Lakes Region of North America, *Atmos. Chem. Phys.*, 12, 7117-7133, doi:  
802 10.5194/acp-12-7117-2012, 2012.

803

804 Holmes, C. D., Jacob, D. J., Mason, R. P., and Jaffe, D. A.: Sources and deposition of reactive gaseous  
805 mercury in the marine atmosphere, *Atmos. Environ.*, 43, 2278-2285, doi:  
806 10.1016/j.atmosenv.2009.01.051, 2009.

807

808 Holmes, C. D., Jacob, D. J., Corbitt, E. S., Mao, J., Yang, X., Talbot, R., Slemr, F.: Global atmospheric model  
809 for mercury including oxidation by bromine atoms, *Atmos. Chem. Phys.*, 10, 12037-12057, 2010.

810 Huang, J.Y., Lyman, S.N., Hartman, J.S., Gustin, M.S.: A review of passive sampling systems for ambient  
811 air mercury measurements, *Environ. Sci.-Processes & Impacts*, 16, 374-392, 2014.

812

813 Huang, J.Y., Miller, M.B., Weiss-Penzias, P., Gustin, M.S.: Comparison of Gaseous Oxidized Hg Measured  
814 by KCl-Coated Denuders, and Nylon and Cation Exchange Membranes, *Environ. Sci. Technol.*, 47, 7307-  
815 7316, 2013.

816

817 Huang, J., Gustin, M.S. Impacts of relative humidity on GOM measurements, submitted to EST

818

819 Huang, J., Gustin, M.S.: Use of passive sampling methods and models to understand sources of mercury  
820 deposition to high elevation sites in the Western United States, 49 (432-441)DOI  
821 10.1021/es502836w, 2015.

822

823 Huang, J., Miller, M.B., Edgerton, E., Gustin, M.S.: Use of Criteria Pollutants, Active and Passive Mercury  
824 Sampling, and Receptor Modeling to Understanding the Chemical Forms of Gaseous Oxidized Mercury in  
825 Florida, this issue.

826

827 Jaffe, D., Prestbo, E., Swartzendruber, P., Weiss-Penzias, P., Kato, S., Takami, A., Hatakeyama, S., Kajii, Y.:  
828 Export of atmospheric mercury from Asia, *Atmos. Environ.*, 39, 3029-3038,  
829 doi:10.1016/j.atmosenv.2005.01.030, 2005.

830

831 Jaffe, D. A., Lyman, S., Amos, H. M., Gustin, M. S., Huang, J., Selin, N. E., Levin, L., ter Schure, A., Mason,  
832 R. P., Talbot, R., Rutter, A., Finley, B., Jaeglé, L., Shah, V., McClure, C., Ambrose, J., Gratz, L., Lindberg, S.,  
833 Weiss-Penzias, P., Sheu, G.-R., Feddersen, D., Horvat, M., Dastoor, A., Hynes, A. J., Mao, H., Sonke, J. E.,  
834 Slemr, F., Fisher, J. A., Ebinghaus, R., Zhang, Y., and Edwards, G.: Progress on Understanding  
835 Atmospheric Mercury Hampered by Uncertain Measurements, *Environ. Sci. Technol.*, doi:  
836 10.1021/es5026432, 2014.

837 Keeler, G., Glinsorn, G., Pirrone, N.: Particulate mercury in the atmosphere: Its significance, transport,  
838 transformation and sources, *Water Air Soil Poll.*, 80, 159-168, 1995.

839

840 Kos, G., Ryzhkov, A., Dastoor, A., Narayan, J., Steffen, A., Ariya, P. A., and Zhang, L.: Evaluation of  
841 discrepancy between measured and modelled oxidized mercury species, *Atmos. Chem. Phys.*, 13, 4839-  
842 4863, doi: 10.5194/acp-13-4839-2013, 2013.

843 Landis, M.S., Stevens, R.K., Schaedlich, F., Prestbo, E.M.: Development and characterization of an  
844 annular denuder methodology for the measurement of divalent inorganic reactive gaseous mercury in  
845 ambient air, *Environ. Sci. Technol.*, 36, 3000-3009, 2002.

846 Landis, M.S., Ryan, J.F., Arnout, F.H., Schure, T., Laudal, D.: The Behavior of Mercury Emissions from a  
847 Commercial Coal-Fired Power Plant: The Relationship Between Stack Speciation and Near-Field Plume  
848 Measurements, *Environ. Sci. Technol.*, 48 (22), 13540-13548, 2015.

849 Laurier , F. J. G.and Mason, R.P.: Mercury concentration and speciation in the coastal and open ocean  
850 boundary layer, *Journal of Geophysical Research*,112, D06302 DOI: 10.1029/2006JD007320) 2007.

851 Laurier, F.J. G., Mason,R.P., Whalin, L., Kato,S.: Reactive gaseous mercury formation in the North Pacific  
852 Ocean's marine boundary layer: A potential role of halogen chemistry, *Journal of Geophysical Research*,  
853 108, 108, D17, 429 DOI: 10.1029/2003JD003625), 2003.

854 Lin, C-J., Pongprueksa, P., Lindberg, S.E., Pehkonen, S.O., Byun, D., Jang, C.: Scientific uncertainties in  
855 atmospheric mercury models I: Model science evaluation, *Atmos. Environ.*, 40, 2911-2928, 2006.

856 Lindberg, S. E.: Mercury partitioning in a power plant plume and its influence on atmospheric removal  
857 mechanisms, *Atmos. Environ.*, 14, 227-231, 1980.

858

859 Lindberg, S. E., Jackson, D. R., Huckabee, J. W., Janzen, S. A., Levin, M. J., Lund, J. R.: Atmospheric  
860 emission and plant uptake of mercury from agricultural soils near the Almaden mercury mine, *J. Environ.*  
861 *Qual.*, 8, 572-578, 1979.

862

863 Lindberg, S. E., Turner, R. R.: Mercury emissions from chlorine production solid waste deposits, *Nature*,  
864 268, 133-136, 1977.

865 Lindberg, S.E., Bullock, R., Ebinghaus, R., Engstrom, D., Feng, X., Fitzgerald, W., et al.: A synthesis of  
866 progress and uncertainties in attributing the sources of mercury in deposition, *AMBIO*, 36, 19-32, 2007.

867

868 Lindberg, S.E., Stratton, W.J.: Atmospheric mercury speciation: Concentrations and behavior of reactive  
869 gaseous mercury in ambient air, *Environ. Sci. Technol.*, 32, 49-57, 1998.

870

871 Lindberg, S.E., Stratton, W.J., Pai, P., Allan, M.A.: Measurements and modeling of a water soluble gas-  
872 phase mercury species in ambient air, *Fuel Process. Technol.*, 65, 143-156, 2000.

873

874 Lohman, K., Seigneur, C., Edgerton, E., and Jansen, J.: Modeling mercury in power plant plumes, *Environ.*  
875 *Sci. Technol.*, 40, 3848-3854, doi: 10.1021/es051556v, 2006.

876

877 Lyman, S. N., and Jaffe, D. A.: Formation and fate of oxidized mercury in the upper troposphere and  
878 lower stratosphere, *Nat. Geosci.*, 5, 114-117, doi: 10.1038/ngeo1353, 2012.

879

880 Lyman, S.N., Jaffe, D.A., Gustin, M.S.: Release of mercury halides from KCl denuders in the presence of  
881 ozone, *Atmos. Chem. Phys.*, 10, 8197-8204, 2010a.

882

883 Lyman, S.N., Gustin, M.S., Prestbo, E.M.: A passive sampler for ambient gaseous oxidized mercury  
884 concentrations, *Atmos. Environ.*, 44, 246-252, 2010b.

885

886 Lyman, S.N., Gustin, M.S., Prestbo, E.M., Kilner, P.I., Edgerton, E., Hartsell, B.: Testing and Application of  
887 Surrogate Surfaces for Understanding Potential Gaseous Oxidized Mercury Dry Deposition, *Environ. Sci.*  
888 *Technol.*, 43, 6235-6241, 2009.

889

890 Lyman, S.N., Gustin, M.S., Prestbo, E.M., Marsik, F.J.: Estimation of dry deposition of atmospheric  
891 mercury in Nevada by direct and indirect methods, *Environ. Sci. Technol.*, 41, 1970-1976, 2007.

892

893 Lyman, S.N., Jaffe, D.A.: Formation and fate of oxidized mercury in the upper troposphere and lower  
894 stratosphere, *Nature Geosci.*, 5, 114-117, 2012.

895

896 Lynam, M.M., Keeler, G.J.: Artifacts associated with the measurement of particulate mercury in an urban  
897 environment: The influence of elevated ozone concentrations, *Atmos. Environ.*, 39, 3081-3088, 2005.

898

899 Malcolm, E.G., Keeler, G.J.: Evidence for a sampling artifact for particulate-phase mercury in the marine  
900 atmosphere, *Atmos. Environ.*, 41, 3352-3359, 2007.

901 McClure, C. D., Jaffe, D. A., Edgerton, E.S.: Evaluation of the KCl Denuder Method for Gaseous Oxidized  
902 Mercury using HgBr<sub>2</sub> at an In-Service AMNet Site, *Environ. Sci. Technol.*, 48 (19), 11437-11444, 2014.

903 Munthe, J., Schroeder, W.H., Xiao, Z., Lindqvist, O.: Removal of gaseous mercury from air using a gold  
904 coated denuder, *Atmos. Environ. Part A. General Topics*, 24, 2271-2274, 1990.

905

906 Murphy, D. M., Hudson, P. K., Thomson, D. S., Sheridan, P. J., and Wilson, J. C.: Observations of mercury-  
907 containing aerosols, *Environ. Sci. Technol.*, 40, 3163-3167, doi: 10.1021/es052385x, 2006.

908

909 Obrist, D., Faïn, X., and Berger, C.: Gaseous elemental mercury emissions and CO<sub>2</sub> respiration rates in  
910 terrestrial soils under controlled aerobic and anaerobic laboratory conditions, *Sci. Total Environ.*, 408,  
911 1691-1700, doi: 10.1016/j.scitotenv.2009.12.008, 2010.

912 Peterson, C., Alishahi, M., Gustin, M.S.: Testing the use of passive sampling systems for understanding  
913 air mercury concentrations and dry deposition across Florida, USA, *Sci. Total Environ.*, 424, 297-307,  
914 2012.

915

916 Pierce, A., Obrist, D., Moosmuller, H., Fain, X., Moore, C.: Cavity ring-down spectroscopy sensor  
917 development for high-time-resolution measurements of gaseous elemental mercury in ambient air,  
918 *Atmos. Measure. Techniques.*, 6, 1477-1489, 2013.

919

920 Pirrone, N., Aas, W., Cinnirella, S., Ebinghaus, R., Hedgecock, I.M., Pacyna, J., et al.: Toward the next  
921 generation of air quality monitoring: Mercury, *Atmos. Environ.*, 80, 599-611, 2013.

922

923 Poissant L., Pilote M., Beauvais C., Constant P., Zhang H.H.: A year of continuous measurements of three  
924 atmospheric mercury species (GEM, RGM and Hg-p) in southern Quebec, Canada. *Atmos. Environ.* 39:  
925 1275-1287, 2005.

926

927 Pongprueksa, P., Lin, C. J., Lindberg, S. E., Jang, C., Braverman, T., Bullock, O. R., Ho, T. C., and Chu, H.  
928 W.: Scientific uncertainties in atmospheric mercury models III: Boundary and initial conditions, model  
929 grid resolution, and Hg(II) reduction mechanism, *Atmospheric Environment*, 42, 1828-1845, doi:  
930 10.1016/j.atmosenv.2007.11.020, 2008.

931  
932 Rutter, A.P., Shakya, K.M., Lehr, R., Schauer, J.J., Griffin, R.J.: Oxidation of gaseous elemental mercury in  
933 the presence of secondary organic aerosols, *Atmos. Environ.*, 59, 86-92, 2012.  
934  
935 Rutter, A.P., Hanford, K.L., Zwiers, J.T., Perillo-Nicholas, A.L., Schauer, J.J., Olson, M.L.: Evaluation of an  
936 offline method for the analysis of atmospheric reactive gaseous mercury and particulate mercury, *J. Air*  
937 *Waste Manag. Assoc.*, 58, 377-383, 2008.  
938  
939 Rutter, A. P., and Schauer, J. J.: The impact of aerosol composition on the particle to gas partitioning of  
940 reactive mercury, *Environ. Sci. Technol.*, 41, 3934-3939, doi: 10.1021/es062439i, 2007a.  
941  
942 Rutter, A. P., and Schauer, J. J.: The effect of temperature on the gas-particle partitioning of reactive  
943 mercury in atmospheric aerosols, *Atmos. Environ.*, 41, 8647-8657, doi:  
944 10.1016/j.atmosenv.2007.07.024, 2007b.  
945  
946 Sather, M.E., Mukerjee, S., Allen, K.L., Smith, L., Mathew, J., Jackson, C., et al.: Gaseous Oxidized  
947 Mercury Dry Deposition Measurements in the Southwestern USA: A Comparison between Texas, Eastern  
948 Oklahoma, and the Four Corners Area, *Sci. World J.*, **Accession Number:** WOS:000334852000001, 2014.  
949  
950 Sather, M.E., Mukerjee, S., Smith, L., Mathew, J., Jackson, C., Callison, R., et al.: Gaseous oxidized  
951 mercury dry deposition measurements in the Four Corners area and Eastern Oklahoma, U.S.A., *Atmos.*  
952 *Poll. Research*, 4, 168-180, 2013.  
953  
954 Schroeder, W.H., Munthe, J.: Atmospheric mercury--An overview, *Atmos. Environ.*, 32, 809-822, 1998.  
955  
956 Schuster, P.F., Krabbenhoft, D.P., Naftz, D.L., Cecil, L.D., Olson, M.L., Dewild, J.F., et al.: Atmospheric  
957 mercury deposition during the last 270 years: A glacial ice core record of natural and anthropogenic  
958 sources, *Environ. Sci. Technol.*, 36, 2303-2310, 2002.  
959  
960 Selin, N. E., Jacob, D. J., Park, R. J., Yantosca, R. M., Strode, S., Jaegle, L., and Jaffe, D.: Chemical cycling  
961 and deposition of atmospheric mercury: Global constraints from observations, *J. Geophys. Res.*, 112, 14,  
962 D02308, doi: 10.1029/2006jd007450, 2007.  
963  
964 Selin, N. E., and Jacob, D. J.: Seasonal and spatial patterns of mercury wet deposition in the United  
965 States: Constraints on the contribution from North American anthropogenic sources, *Atmos. Environ.*,  
966 42, 5193-5204, 2008.  
967  
968 Sheu, G.R., Mason, R.P.: An examination of methods for the measurements of reactive gaseous mercury  
969 in the atmosphere, *Environ. Sci. Technol.*, 35, 1209-1216, 2001.  
970  
971 Sholupov, S., Pogarev, S., Ryzhov, V., Mashyanov, N., Stroganov, A.: Zeeman atomic absorption  
972 spectrometer RA-915+for direct determination of mercury in air and complex matrix samples, *Fuel*  
973 *Process. Technol.*, 85, 473-485, 2004.  
974  
975 Skov, H., Sørensen, B.T., Landis, M.S., Johnson, M.S., Sacco, P., Goodsite, M.E., et al.: Performance of a  
976 new diffusive sampler for Hg0 determination in the troposphere, *Environ. Chem.*, 4, 75-80, 2007.  
977

976 Slemr, F., Weigelt, A., Ebinghaus, R., Brenninkmeijer, C., Baker, A., Schuck, T., Rauthe-Schoch, A., Riede,  
977 H., Leedham, E., Hermann, M., van Velthoven, P., Oram, D., O'Sullivan, D., Dyrhoff, C., Zahn, A., and  
978 Ziereis, H.: Mercury Plumes in the Global Upper Troposphere Observed during Flights with the CARIBIC  
979 Observatory from May 2005 until June 2013, *Atmosphere*, 5, 342-369, doi: 10.3390/atmos5020342,  
980 2014.

981 Slemr, F., Brunke, E.G., Ebinghaus, R., Kuss, J.: Worldwide trend of atmospheric mercury since 1995.  
982 *Atmos. Chem. Phys.*, 11, 4779-4787, 2011.

983

984 Soerensen, A. L., Jacob, D. J., Streets, D. G., Witt, M. L. I., Ebinghaus, R., Mason, R. P., Andersson, M.,  
985 Sunderland, E. M.: Multi-decadal decline of mercury in the North Atlantic atmosphere explained by  
986 changing subsurface seawater concentrations, *Geophys. Res. Lett.*, 39, L21810,  
987 doi:10.1029/2012GL053736, 2012.

988

989 Sprovieri, F., Pirrone, N., Gardfeldt, K., Sommar, J., Mercury speciation in the marine boundary layer  
990 alonga 6000 km cruise path around the Mediterranean Sea, *AE*, 37, 63-71, 2003.

991

992 Steffen, A., Lehnher, I., Cole, A., Ariya, P., Dastoor, A., Durnford, D., Kirk, J., Pilote, M. Atmospheric  
993 mercury measurements in the Canadian Arctic Part 1: A review of recent field measurements, *Science of  
994 the Total Environment*, 509-510 3-15, 2015.

995 Steffen, A., Scherz, T., Olson, M., Gay, D., Blanchard, P.: A comparison of data quality control protocols  
996 for atmospheric mercury speciation measurements, *Environ. Monit.*, 14, 752-765, 2012.

997

998 Steffen, A., Bottenheim, J., Cole, A., Ebinghaus, R., Lawson, G., and Leaitch, W. R.: Atmospheric mercury  
999 speciation and mercury in snow over time at Alert, Canada, *Atmos. Chem. Phys.*, 14, 2219-2231, doi:  
1000 10.5194/acp-14-2219-2014, 2014.

1001 Stratton, W.J., and Lindberg, S.E.: Use of a refluxing mist chamber for measurements of gas phase  
1002 mercury(II) species in the atmosphere, *Water Air Soil Pollut.*, 80, 1269-  
1003 1278, 1995.

1004

1005 Stratton, W.J., Lindberg, S.E., Perry, C.J.: Atmospheric mercury speciation: Laboratory and field  
1006 evaluation of a mist chamber method for measuring reactive gaseous mercury, *Environ. Sci. Technol.*,  
1007 35, 170-177, 2001.

1008

1009 Syrakov, D. and Gryning, S.E., Schiermeier, F.A. (Eds.): On a PC-oriented Eulerian Multi-level model for  
1010 long-term calculations of the regional sulphur deposition., *Air pollution modeling and its application*, XI,  
1011 21, Plenum Press, New York, 645-6, 1995.

1012 Swartzendruber, P. C., Jaffe, D. A., and Finley, B.: Development and First Results of an Aircraft-Based,  
1013 High Time Resolution Technique for Gaseous Elemental and Reactive (Oxidized) Gaseous Mercury,  
1014 *Environ. Sci. Technol.*, 43, 7484-7489, doi: 10.1021/es901390t, 2009.

1015

1016 Talbot, R., Mao, H.; Scheuer, E., Dibb, J., Avery, M.; Browell, E., Sachse, G., Vay, S., Blake, D., Huey, G.,  
1017 Fuelberg, H. Factors influencing the large-scale distribution of  $Hg^{\circ}$  in the Mexico City area  
1018 and over the North Pacific. *Atmos. Chem. Phys.*, 8, 2103-2114 2008.

1019

1020 Talbot, R., Mao, H.T., Feddersen, D., Smith, M., Kim, S.Y., Sive, B., et al.: Comparison of Particulate  
1021 Mercury Measured with Manual and Automated Methods, *Atmosphere*, 2, 1-20, 2011.

1022

1023 Temme, C., Einax Jr., W., Ebinghaus, R., and Schroeder, W.H.: Measurements of Atmospheric Mercury  
1024 Species at a Coastal Site in the Antarctic and over the South Atlantic Ocean during Polar Summer,  
1025 *Environ. Sci. Technol.*, 37, 22-31, 2002.

1026

1027 Timonen, H., Ambrose, J. L., and Jaffe, D. A.: Oxidation of elemental Hg in anthropogenic and marine  
1028 airmasses, *Atmospheric Chemistry and Physics*, 13, 2827-2836, doi: 10.5194/acp-13-2827-2013, 2013.

1029

1030 Tong, Y. D., Eichhorst, T., Olson, M. R., Rutter, A. P., Shafer, M. M., Wang, X. J., and Schauer, J. J.:  
1031 Comparison of heterogeneous photolytic reduction of Hg(II) in the coal fly ashes and synthetic aerosols,  
1032 *Atmos. Res.*, 138, 324-329, doi: 10.1016/j.atmosres.2013.11.015, 2014.

1033

1034 Travnikov, O., Lin, C. J., Dastoor, A., Bullock, O. R., Hedgecock, I., Holmes, C., Ilyin, I., Jaegle, L., Jung, G.,  
1035 Pan, L., Pongprueksa, P., Ryzhkov, A., Seigneur, C., and Skov, H.: Global and Regional Modeling, in:  
1036 Hemispheric Transport of Air Pollution. Part B: Mercury, edited by: Pirrone, N., and Keating, T., United  
1037 Nations, 97-144, 2010.

1038 Travnikov, O. and Ilyin I., Pirrone N. and Mason, R. (Eds.): The EMEP/MSC-E mercury modeling system,  
1039 In: Mercury fate and transport in the global atmosphere, Springer, 571-587, 2009.

1040

1041 UNEP Minamata Convention on Mercury, <http://www.mercuryconvention.org/>, accessed: 10/15/2014,  
1042 2014.

1043

1044 Urba, A., Kvietkus, K., Sakalys, J., Xiao, Z., Lindqvist, O.: A new sensitive and portable mercury vapor  
1045 analyzer GARDIS-1A. *Water Air and Soil Pollution*, 80, 1305-1309, 1995.

1046 Vijayaraghavan, K., Karamchandani, P., Seigneur, C., Balmori, R., and Chen, S. Y.: Plume-in-grid modeling  
1047 of atmospheric mercury, *J. Geophys. Res.*, 113, 12, D24305, doi: 10.1029/2008jd010580, 2008.

1048

1049 Wang, Y.G., Huang, J.Y., Hopke, P.K., Rattigan, O.V., Chalupa, D.C., Utell, M.J., et al.: Effect of the  
1050 shutdown of a large coal-fired power plant on ambient mercury species, *Chemosphere*, 92, 360-367,  
1051 2013.

1052

1053 Weiss-Penzias, P., Jaffe, D.A., McClintick, A., Prestbo, E.M., Landis, M.S.: Gaseous elemental mercury in  
1054 the marine boundary layer: Evidence for rapid removal in anthropogenic pollution, *Environ. Sci.*  
1055 *Technol.*, 37, 3755-3763, 2003.

1056

1057 Wright, G., Woodward, C., Peri, L., Weisberg, P.J., Gustin, M.S.: Application of tree rings  
1058 dendrochemistry for detecting historical trends in air Hg concentrations across multiple scales,  
1059 *Biogeochem.*, 120, 149-162, 2014a.

1060

1061 Wright, G., Gustin, M.S., Weiss-Penzias, P., Miller, M.B.: Investigation of mercury deposition and  
1062 potential sources at six sites from the Pacific Coast to the Great Basin, U.S.A., *Sci. Total Environ.*, 470,  
1063 1099-1113, 2014b.

1064

1065 Xiao, Z.F., Munthe, J., Lindqvist, O.: Sampling and determination of gaseous and particulate mercury in  
1066 the atmosphere using gold-coated denuders, *Water Air Soil Poll.*, 56, 141-151, 1991.

1067

1068 Zhang, W., Tong, Y.D., Hu, D., Ou, L.B., Wang, X.J.: Characterization of atmospheric mercury  
1069 concentrations along an urban-rural gradient using a newly developed passive sampler, *Atmos. Environ.*,  
1070 47, 26-32, 2012.

1071

1072 Zhang, Y., Jaegle, L., van Donkelaar, A., Martin, R.V., Holmes, C.D., Amos, H.M., et al.: Nested-grid  
1073 simulation of mercury over North America, *Atmos. Chem. Phys.*, 12, 6095-6111, 2013.

1074

**Table captions.**

Table 1. Pros and cons of automated and passive methods used to make Hg measurements.

Table 2. Regression equations comparing nylon membrane and cation exchange membrane measured GOM concentrations versus those measured by the denuder using the University of Nevada, Reno (UNR) laboratory manifold system and charcoal scrubbed air.

Table 3. Atmospheric models with speciated mercury .

**Figure captions.**

Figure 1. Correlation between GOM concentrations measured by KCl-coated denuder versus the nylon and cation exchange membranes in activated charcoal scrubbed air. Modified from Huang et al. (2013).

Figure 2. Thermal desorption profiles generated by permeating different Hg compounds. Modified from Huang et al. (2013). Percent indicates the amount released relative to the total. Profiles were developed in activated charcoal scrubbed air. Compounds being permeated may not be the exact compound in the permeation tube, and this needs to be verified.

Figure 3. Figure 7 from Weiss-Penzias et al. (2003). Reprinted with permission from Weiss-Penzias et al. 2003, Copyright 1 September 2003 American Chemical Society.

Table 1. Pros and cons of automated and integrative methods used to make Hg measurements.

	<b>Hg form measured/detection limit</b>	<b>Pros</b>	<b>Cons</b>	<b>Suggestion/comments</b>
<b>Automated</b>				
Tekran 2537-gold traps	GEM or TGM 0.5 ng m <sup>-3</sup> ambient air	Low detection limit, 2.5 to 5 minute resolution, there is a calibration source, standardized by AMNet and CAMNet	Inlet configuration will impact whether measuring GEM or TGM Requires fairly trained technicians, stable	Suggest using a pyrolyzer at the inlet if TAM measurement is desired.

		(cf. Prestbo and Gay, 2009)	electrical source, regular calibration and checks	
Tekran 1130-KCl denuder	GOM 1 pg m <sup>-3</sup>	Good time resolution (1 to 2 hours)	No calibration source, coating denuders needs to be done by one operator, does not measure all the GOM in air	New method needs to be developed that measures all forms in air and is not impacted by relative humidity and ozone. A different denuder coating would be useful.
Tekran 1135-quartz filter and chips	PBM 1 pg m <sup>-3</sup>	Good time resolution (1 to 2 hours)	Positive artifact due to measurement of GOM that passes through the denuder, not all PBM is measured due to select grain size capture	Filter method may be best and suggest using cation exchange membranes
Lumex	GEM or TGM in air Total Hg in liquids and solids <1 ng m <sup>-3</sup> for air if averaged over 5 minutes	Good time resolution (seconds) Field portable Allows for measurement of Hg concentrations in environmental media in the field	Older version has issues with stability. See SI.	Good for industrial and field applications
Gardias	GEM or TGM 0.5 ng m <sup>-3</sup>	Good time resolution (2.5 minutes)	Requires trained operators	
DOHGS	GEM and TGM 80 pg m <sup>-3</sup>	Good time resolution (2.5 minutes)	Requires highly trained operators and stable environment	Useful as a research instrument
Laser	GEM	Fast time resolution	Requires highly trained	Useful as research instrument

		(seconds)	operators and a stable environment,	Could be configured to measure RM and GEM
<b>Manual Active</b>				
GOM Mist Chamber	GOM Blank: 20-50 pg		Complicated operation Need acidified solution	Useful as a research instrument, needs to be re-evaluated
Direct Particulate Matter Sampler Measurement	PBM Probably GOM	Easy operation	Artifacts from GOM partition, choice of filters important to consider as well as length of sampling line and collection time	
UNR Active System	GOM ~30 pg m <sup>-3</sup>	Easy operation, Useful for quantifying GOM and the chemical forms in air.	Potentially some PBM measured	Good for networks, and it could be used to help calibrate measurements made by the Tekran.
<b>Manual Passive systems</b>				
GEM Passive Sampler	GEM or TGM 10-80 pg m <sup>-3</sup>	Easy operation	Long time resolution	Good for worldwide network
GOM Passive sampler-concentration	GOM 2.3-5 pg m <sup>-3</sup>	Easy operation	Long time resolution	Needs a new design
GOM Passive sampler-deposition	GOM Minor PBM 0.02-0.24 pg m <sup>-2</sup> h <sup>-1</sup>	Easy operation Real Hg loading to ecosystem	Long time resolution	Good for worldwide network

Table 2. Regression equations comparing nylon membrane and cation exchange membrane measured GOM concentrations versus those measured by the denuder using the UNR laboratory manifold system and charcoal scrubbed air.

	HgCl <sub>2</sub>	HgBr <sub>2</sub>	HgO	Hg(NO <sub>3</sub> ) <sub>2</sub>	HgSO <sub>4</sub>
Nylon membrane (y)	y=1.6x +0.002	y=1.7x +0.01 r <sup>2</sup> =0.99, n=10	y=1.8x +0.02 r <sup>2</sup> =0.99, n=8	y=1.4x +0.04 r <sup>2</sup> =0.90, n=12	y=1.9x -0.1 r <sup>2</sup> =0.6, n=12
KCl denuder (x)	n=12				
Cation- exchange membrane (y)	y=2.4x +0.1 r <sup>2</sup> =0.58, n=9	y=1.6x+0.2 r <sup>2</sup> =0.86, n=5	y=3.7x +0.1 r <sup>2</sup> =0.99, n=6	y=12.6x -0.02 r <sup>2</sup> =0.50, n=6	y=2.3x +0.01 r <sup>2</sup> =0.95, n=18
KCl denuder (x)					

Table 3. Atmospheric models with speciated mercury

Model Name	Domain	Type	Explicit or lumped Hg(II)	References
GRAHM	Global	3D, Eulerian	Explicit (HgCl <sub>2</sub> , HgO)	Dastoor & Larocque [2004]; Ryaboshopka et al. [2007a,b]; Dastoor et al. [2008]; Durnford et al. [2010]; Kos et al. [2013]; Dastoor et al. [2014]
GEOS-Chem	Global <sup>a</sup>	3D, Eulerian	Bulk Hg(II)	Selin et al. [2008]; Selin & Jacob [2008]; Holmes et al. [2010]; Corbitt et al., [2011]; Amos et al., [2012]; Zhang et al., [2012]; Chen et al. [2014]; Kikuchi et al [2013]
CMAQ-Hg	Continental US	3D, Eulerian	Explicit (HgCl <sub>2</sub> , HgO)	Bullock & Brehme [2002]; Vijayaraghavan et al. [2008]; Holloway et al. [2012]; Bash et al. [2014]
GLEMOS	Variable, global to regional	3D, Eulerian	Lumped	Travnikov & Ryaboshapko (2002, EMEP report); Travnikov (2010)
ECHMERIT	Global	3D, Eulerian	HgO <sub>(g)</sub> , HgCl <sub>2(g)</sub> , lumped Hg(II) <sub>(aq)</sub>	De Simone et al., (2014); Jung et al. (2009)
WRF-Chem	Regional	3D, Eulerian	Lumped	Gencarellia et al 2014
MSCE-Hg- Hem	Northern Hemisphere	3D, Eulerian	HgO <sub>(g)</sub> , HgCl <sub>2(g)</sub> , lumped Hg(II) <sub>(aq)</sub>	Travnikov and Ryaboshapko (2002); Travnikov (2005); Travnikov O. and Ilyin I. (2009)
ADOM	North America, Europe	3D, Eulerian	HgO <sub>(g)</sub> , HgCl <sub>2(g)</sub> , lumped Hg(II) <sub>(aq)</sub>	Petersen et al. (2001)
DEHM	Northern Hemisphere	3D, Eulerian	HgO <sub>(g)</sub> , HgCl <sub>2(g)</sub> , lumped Hg(II) <sub>(aq)</sub>	Christensen et al. (2004); Skov et al. (2004, EST)
WoRM3	Global	2D, Multi- media	Lumped	Qureshi et al. (2011)

PHANTAS	Arctic	Box model	Detailed, explicit Hg(II) compounds	Toyota et al. (2014)
HYSPPLIT	Global	3D, Lagrangian	$\text{HgO}_{(g)}$ , $\text{HgCl}_{2(g)}$ , lumped $\text{Hg(II)}_{(aq)}$	Cohen et al. 2004
TEAM	North America	3D, Eulerian	$\text{HgO}_{(g)}$ , $\text{HgCl}_{2(g)}$ , lumped $\text{Hg(II)}_{(aq)}$	Bullock et al. 2008; 2009
CTM-Hg	Global	3D, Eulerian	$\text{HgO}_{(g)}$ , $\text{HgCl}_{2(g)}$ , lumped $\text{Hg(II)}_{(aq)}$	Shia et al 1999; Seigneur et al. 2001; 2004; 2003; 2006; Lohman et al., 2008
REMSAD	North America	3D, Eulerian	Explicit ( $\text{HgCl}_2$ , $\text{HgO}$ )	Bullock et al. 2008; 2009
EMAP	Europe	3D, Eulerian	Lumped	Syrakov et al., 1995

<sup>a</sup> The standard GEOS-Chem has a global domain with the option to have a nested high-resolution simulation over North America [Zhang et al., 2012]

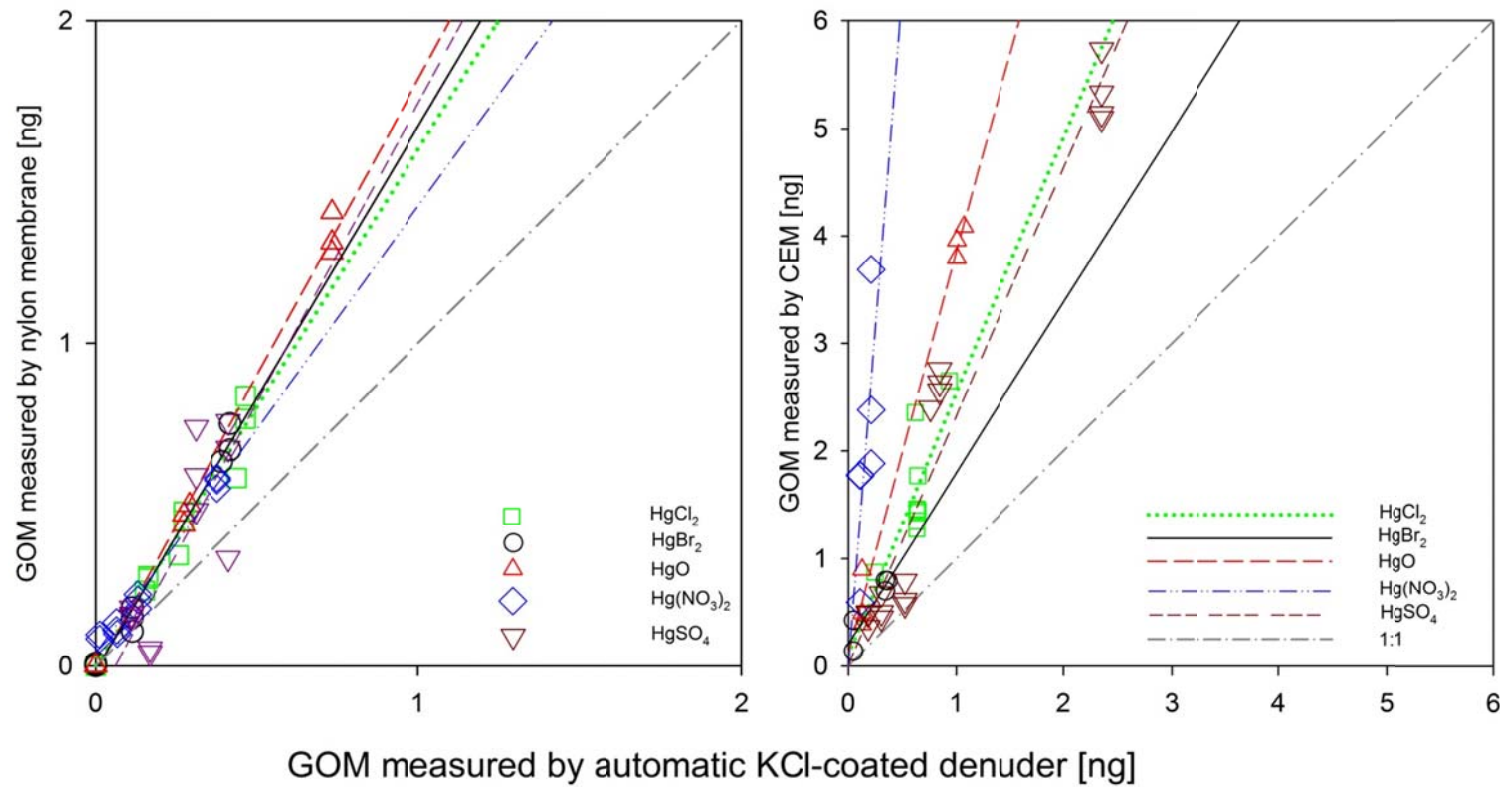


Figure 1. Correlation between GOM concentrations measured by KCl-coated denuder versus the nylon and cation exchange membranes in activated charcoal scrubbed air. Modified from Huang et al. (2013).

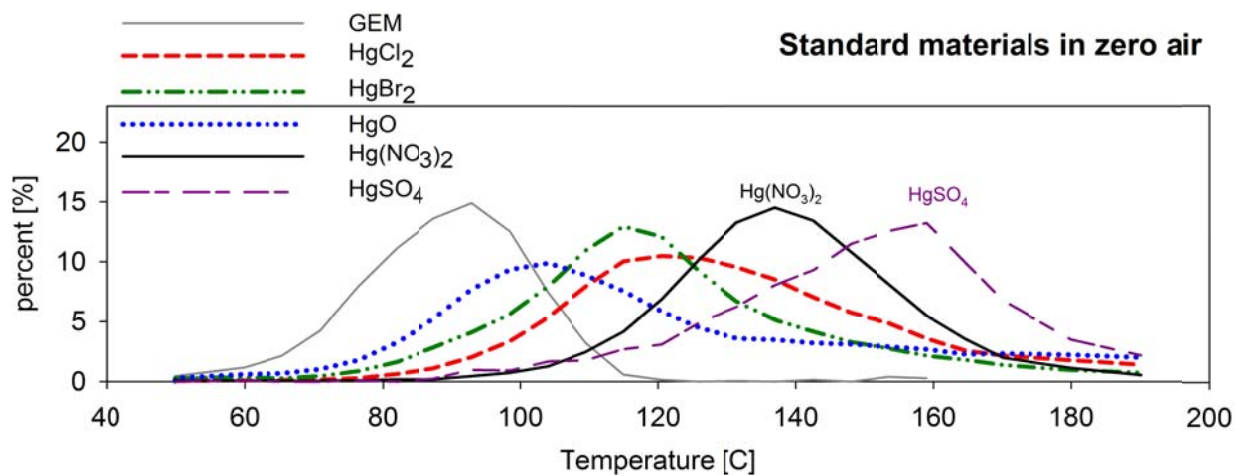


Figure 2. . Thermal desorption profiles generated by permeating different Hg compounds. Modified from Huang et al. (2013). Percent indicates the amount released relative to the total. Profiles were developed in activated charcoal scrubbed air. Compounds being permeated may not be the exact compound in the permeation tube and this needs to be verified.

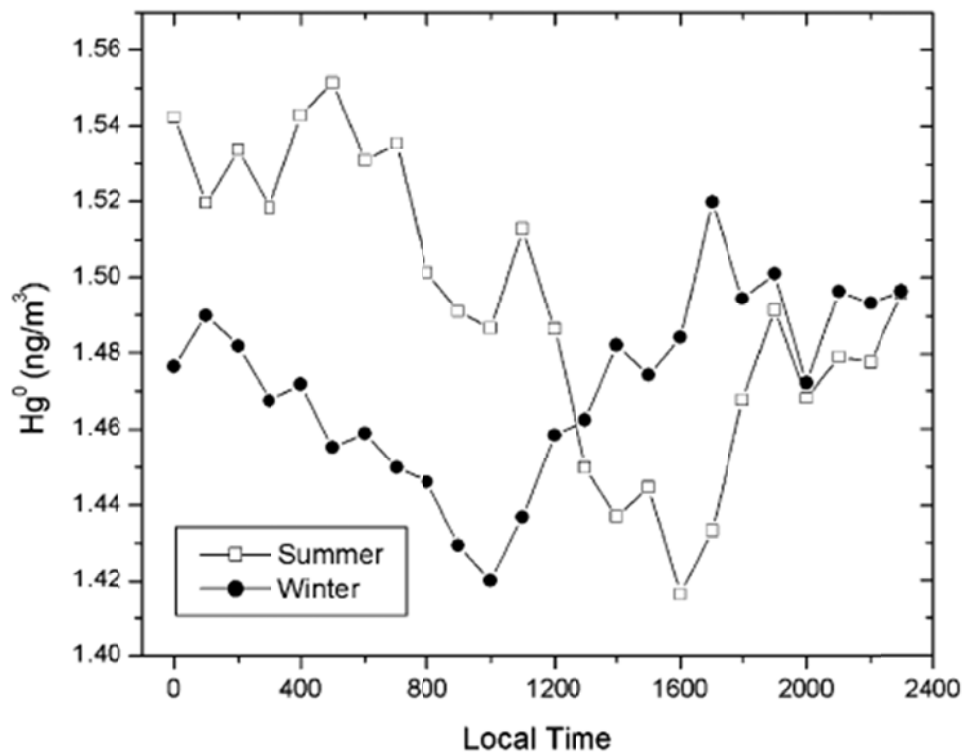


Figure 3. Figure 7 from Weiss-Penzias et al. (2003). Reprinted with permission from Weiss-Penzias et al. 2003, Copyright 1 September 2003 American Chemical Society.